UNIVERSITY OF CINCINNATI

March 1st , 19 99

I, Yuelei Yang ,

hereby submit this as part of the requirements for the degree of:

Master of Science

in Mechanical Engineering

It is entitled A Drying Model of a Vibro-Separator

Approved by:

Dr. F. Gerner Frank M. Gerner

Dr. A. Hazrati Azar M. Hazrati

Dr. M. Kazmierczak Michael Kazmierczak

A Drying Model of a Vibro-Separator

A thesis submitted to the

Division of Research and Advanced Studies
of the University of Cincinnati

in partial fulfillment of the
requirements for the degree of

Master of Science

Department of Mechanical, Industrial and Nuclear Engineering
College of Engineering

1999

by

Yuelei Yang

B.E., Southeast University, China, 1993

Committee Chair: Dr. Frank M. Gerner

Abstract

Vibro-separators are widely used to separate solid particles from slurries and/or to size segregate the dried product. In this thesis, a mathematical model was developed to theoretically evaluate the vacuum drying of the collected solid on the screen of a vibro-separator.

The whole drying process can be divided into two stages: the constant drying rate stage, and the decreasing drying rate stage. The drying rate during the first stage is the evaporating rate of the moisture from the product surface and thus is merely a function of the mass transfer coefficient and humidity differences. However, during the second stage of drying, the evaporating surface moves to the inside of the cake layer and thus the drying rate decreases. In this stage, both evaporation and diffusion control the drying rate. This theoretical model utilizes an energy balance for the drying process and uses thermal parameters to calculate the drying rate.

Experiments were performed, and a comparison is made with the mathematical model. The role of some major factors such as vacuum level, air bleeding rate, critical moisture content of the product, vibration energy transferred to the screen, and the size of the product particles are also discussed. A simple computer program had been written to calculate the drying rate based on the characteristics of the product and processing parameters.

Acknowledgements

Foremost, I would like to express my gratitude to my advisor, Dr. Frank Gerner, for his patience, guidance and tireless review of this thesis. It is his inspiration and support that encourage me to accomplish my work.

Special thanks also go to Dr. Azar Hazrati for her many contributions. Without her help, it is not possible to finish the experimental section of this thesis. Her insightful comments are invaluable and make this thesis stronger.

Thanks also go to Dr. M. Kazmierczak, who takes the time to be on my committee and provides useful suggestions. Thanks are extended to my friends: Xiangdong Liu and Wensheng Xie, for their helps and suggestions. Also, the assistance I received from members of SWECO Test-Laboratory should be noted. They provided a lot of useful data and results to this thesis.

Finally, I would like to say thanks to my parents and sister, who are in the other side of the Pacific Ocean and always the source of encouragement.

Table of Contents

List of Figures

List of Tables

Nomenclature

$\dot{m}$ = drying rate per unit time (kg moisture/s)

L = air bleeding rate (kg dry air/s)

ω_2 = absolute humidity of exit air (kg moisture/ kg dry air)

ω_1 = absolute humidity of inlet air (kg moisture/ kg dry air)

ω = absolute humidity of air (kg moisture/ kg dry air)

p = total pressure of the wet air (Pa)

p_a = partial pressure of the dry air (Pa)

p_v = partial pressure of water vapor (Pa)

ϕ = relative humidity of the wet air (%)

β = mass transfer coefficient (m/s)

h_{fg} = latent heat of water (kJ/kg)

H_s = the specific humidity of the saturated air

(kg moisture/ kg dry air)

H_a = specific humidity of the dry air

(kg moisture/ kg dry air)

A = evaporating/heat transfer surface area (m^2)

ρ = density of the dry air (kg/m^3)

α = heat transfer coefficient. ($W/(m^2K)$)

t = dry-bulb temperature of the air (K)

t_w = wet-bulb temperature of the air (K)

c_s = humid heat of air (m/[s*°C])

k = thermal conductivity of the product (W/(m°C))

τ = Total drying time

G = mass of the dry product. (kg dry product)

X_c = critical moisture content of the product

(kg moisture/ kg dry product)

X = moisture content of the product (kg moisture/kg dry product)

G_G= mass velocity of dry air (kg/[m^{2*}hour])

λ = thermal conductivity of the air (W/[m°C])

u = velocity of the particles (m/s)

d = mean diameter of the wet particles (m)

ν = kinematics viscosity of the air (m^2/s)

s = distance from drying front to solid-air interface (m)

p_s= partial pressure of the vapor in the saturated air (Pa)

i_a = entropy of the dry air (kJ/kg dry air)

i_m = entropy of the moisture (kJ/kg moisture)

$c_{p,air}$ = specific heat of the air (kJ/[kg°C])

$c_{p,moisture}$ = specific heat of the vapor (kJ/[kg°C])

N = total number of the capillary channels

d_c = the mean diameter of the capillary channels (m)

l_e = the effective length (m)

Chapter 1: Introduction

In the pharmaceutical, chemical, food, medical and environmental industries, in many cases, product particles are discharged from the product reactors in the form of dilute slurry. It is necessary to separate solid particles from the slurry and further process the dry powder. Recently developed sanitary separators offer the capability of dewatering/drying the slurry, drying the product on the screen and then discharging the dry powder.

In a typical sanitary separator, the dilute slurry is introduced through the inlet port on the top of the separator. It then passes through a top screen and reach the product screen. The fine particles, which accumulate on the product screen, are in form of wet cake.

Air at atmospheric pressure is introduced from underneath of screen, while vacuum is "pulled" through the top. The air, which is pulled through the product screen by vacuum, picks up the moisture from the product. The lower pressure, created by the vacuum pump, also facilitate evaporation of water. Vibration of the unit during dewatering and drying phase keeps particles suspended above the product screen and thus prevents them from sticking to the screen. At completion of drying of product, dried powder will be discharged through a discharge spout.

1.1 Problem statement

During the drying process, heat is transferred from the purging air that is distributed through the screen openings, to the wet product. This air stream is used to

evaporate moisture content from the product and carry the moisture away from the product cake into the vacuum stream.

The drying process may be controlled by pure evaporation or both evaporation and diffusion. The objective of this thesis research is to make a precise description of the drying process, develop a mathematical model of the drying process, analyze all the factors which affect the drying process, compare the mathematical results with the experiments and provide an application program that can predict the drying time and give some suggestions for optimization.

1.2 Experimental and theoretical methodologies

The most important parameter of the drying process is the drying rate. There are two approaches to obtain this parameter. A simple approach is by direct experimentation. For a given air bleeding rate and inlet air humidity, the drying rate can be predicted:

$$\dot{m} = L(\omega_2 - \omega_1) \tag{1.1}$$

In a practical drying process, the bleeding air rate, L, and inlet air specific humidity, ω_1, may remain as constants, but the exit air humidity ω_2 may change a lot throughout the drying process. If this exit air humidity can be measured, the experimental drying rate can be obtained with Equation (1.1).

The other approach is to theoretically predict the drying rate and the drying time. A parametric study based on a theoretical analysis is used to quantify the drying process in

terms of vacuum level, air-bleeding rate, properties of particles, critical moisture content and other factors. This analysis is based upon a one-dimensional thermal model, where the whole drying process is assumed to be adiabatic. Compared with the experimental approach, this model can predict the drying rate precisely without measuring the exit air humidity as a function of time. A computer program based on this model is also provided. (See details in Chapter 3.)

Chapter 2 will review some background of drying, Chapter 3 will present a mathematical model, Chapter 4 will introduce the experimental procedures, Chapter 5 will explain the results, Chapter 6 will discuss the main factors which influence the drying process and Chapter 7 provides recommendations and conclusions.

Chapter 2 Background

In this chapter, the basic concepts of the drying process will first be described. Then the properties of the product moisture and the wet air will be discussed. Finally, the available convective drying models will be described.

2.1 Basic concepts of the drying process

Drying can be defined as the separation process that the liquid content (usually water) is removed from solids or nearly solid materials. The separation may be carried out in a rough mechanical manner without phase change using filtration, centrifugation, or press out. This kind of mechanical separation is called dewatering. Moisture may also be removed from a moist product by purging dry air or supplying heat. In the following chapters, discussions will concentrate on the thermal drying.

Thermal drying always consists of two steps. First, conduction, convection, or radiation from outside the product supplies heat. This heat is used to evaporate or vaporize the moisture out of the product. Second, the product phase and the steam are separated as follows. Steam is removed from the product and discharged outside of the dryer.

Common thermal drying methods include convection, contact and radiation drying. For special cases, some special drying methods such as vacuum drying, freeze drying and high frequency drying are applied. In this thesis research, only concentration is convective drying processes.

In convective drying processes, wet products are dried with a purging gas. Heat and mass are simultaneously transferred. If the product surface is sufficiently wet, the drying

rate is only a function of the mass and heat transfer at the surface (surface evaporation). If the moisture content in the product is below a critical moisture content, the drying rate is largely controlled by heat transfer and the movement of the moisture inside the product to the surface (drying inside the product).

Mechanical dewatering is usually installed upstream of thermal drying. A typical drying stage consisting of the process units is shown in Figure 2.1. If a moist product with an initial moisture content $X_{p,i}$ (given in kg moisture per kg dry solid), is predried by mechanical means such as centrifugation or filtration to a moisture content $X_{p,1}$, the required cost increases with decreasing $X_{p,1}$. However, the energy input required in the

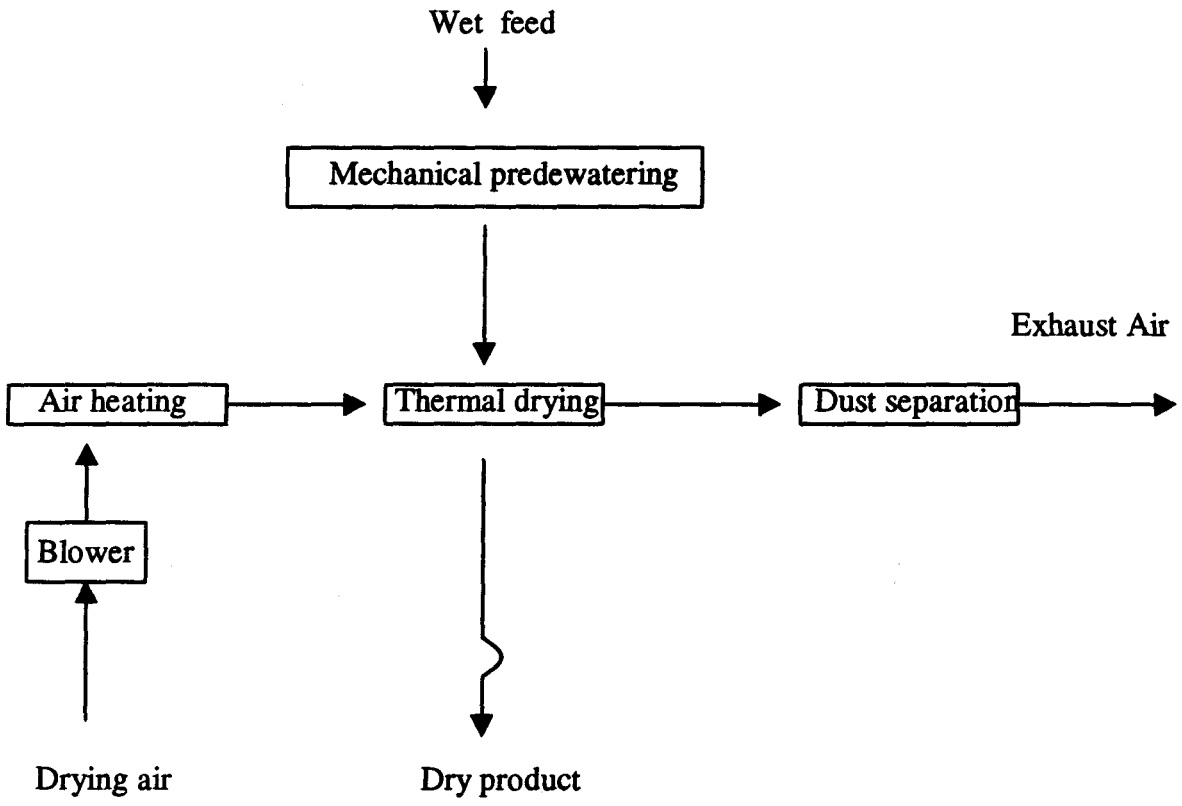

Figure 2.1 Convection drying

subsequent thermal drying increases with increasing $X_{p,1}$. Therefore, the intermediate product moisture content, $X_{p,1}$, has to be adjusted to minimize the total expenditure for the mechanical and thermal drying.

Thermal drying is an important thermal separation technique used in most technical fields, for example, drying of fuel, dyes, foodstuffs and luxury items. Due to the different properties associated with different moist products, it follows that there are many process variations and dryer designs. Mathematical modeling is made difficult or impossible without identifying the characteristics of the moisture product. In the next section, the properties of the product moisture will be discussed.

2.2 Properties of the product moisture

The product to be dried may be characterized as one of following:

- Solid:
  - free flowing (powder, crystalline, fiber, granulate, flake)
  - pieces
  - flat
- Pulp or Paste:
  - high viscosity although able to be pumped (liquid of high viscosity, high viscosity gelatin, muddy)
  - high viscosity, not able to be pumped (thick paste, moldable pastes)
- Liquid:
  - solution

- colloidal solution
- suspension
- slurry

The wet product is a mixture of moisture and dry product particles. It contains moisture mainly in the form of adsorbed liquid, capillary liquid, liquid causing the solid to swell or as bound liquid. Adsorbed liquid is a thin liquid film spread on the outer product surface. The vapor pressure above the liquid film corresponds to its saturation pressure at every temperature. Capillary liquid wets the inner pore surface of a porous solid. During the drying process, the liquid has to be transferred to the air-solid surface where drying happens by capillary forces. With products having macro capillaries of size $> 10^{-7}$ m, the vapor pressure still approximately corresponds to the saturation pressure. With products having microscopic pores $< 10^{-7}$ m, the vapor pressure is lower than the saturation pressure. During the drying process this decreases because the moisture is bonded in the micro capillaries. The solid is termed "hygroscopic". It takes moisture from the surroundings as long as the moisture vapor pressure is equal to the saturation pressure. Swelling liquid not only wets the surface of the product but also causes the solid to swell and becomes part of the structure of the product. Moisture may also be present as water of crystallization. Removing the water of crystallization requires exceeding a crystal decomposition temperature which is specific to the crystal and which is generally not obtained during thermal drying.

If a hygroscopic wet product comes into contact with a vapor mixture containing steam, moisture is adsorbed until the adsorption equilibrium is reached. If, however, the wet product releases steam until the moisture partial pressure in the gas corresponds to

the vapor pressure inside the product. Adsorption and desorption equilibria are described by sorption isotherms, its courses depend on the type of product, the moisture content, and the moisture bond with the product.

The course and time of the drying process depend on the drying conditions, on the temperature and moisture profiles developed during the drying process, and above all, on the moisture movement in the product. The properties, form and dimension of the product and the type of moisture bond in the product govern moisture movement.

2.3 Properties of wet air

The capacity of air for moisture removal depends on its humidity and its temperature. The study of relationships between air and its associated water is called psychrometry.

Air is said to be saturated with water vapor at a given temperature and pressure if its humidity is a maximum under these conditions. If further water is added to saturated air, it must appear as liquid water in the form of a mist or droplets. Under conditions of saturation, the partial pressure of the water vapor in the air is equal to the saturation vapor pressure of water at that temperature.

Humidity is measure of the water content of the air. The absolute or specific humidity is defined as the mass of water vapor per unit mass of dry air:

$$\omega = \frac{m_v}{m_a} \tag{2.1}$$

The specific humidity can be expressed in terms of partial pressures and molecular weights by solving the ideal gas equation of state for m_a and m_v, respectively, and substituting the resulting expressions into Equation (2.1) to obtain

$$\omega = \frac{m_a}{m_v} = \frac{M_v p_v V / RT}{M_a p_a V / RT} = \frac{M_v p_v}{M_a p_a} \tag{2.2}$$

The total pressure of a gasous mixture, such as air and water vapor, is made up from the sum of the pressures of its constituents, which are called the partial pressure. Each partial pressure arises from the molecular concentration of the constituent and the pressure exerted is that which corresponds to the number of moles present and the total volume of the system. The partial pressures are added to obtain the total pressure. For wet air, there is the following relationship:

$$p_a = p - p_v \tag{2.3}$$

Introducing Equation (2.3) into Equation (2.2) and noting that the ratio of the molecular weight of water to that of dry air is approximately 0.622, Equation (2.2) can be written as

$$\omega = 0.622 \frac{p_v}{p - p_v} \tag{2.4}$$

The moisture content of air can also be described in terms of the relative humidity, ϕ, defined as the ratio of the mole fraction of water vapor, y_v, in a given moist air sample

to the mole fraction, $y_{v,sat}$ in a saturated moist air sample at the same mixture temperature and pressure

$$\phi = \frac{y_v}{y_{v,sat}}\Bigg)_{T,p} \tag{2.5}$$

Since

$$p_v = y_v p$$
$$p_{sat} = y_a p$$

The relative humidity can be expressed as

$$\phi = \frac{p_v}{p_{sat}}\Bigg)_{T,p} \tag{2.6}$$

Another useful concept in psychrometry is the wet-bulb temperature, as compared with the ordinary temperature, which is called the dry-bulb temperature. The wet-bulb temperature is usually obtained by following methods: For example, a water surface, such as a thermometer bulb surrounded by a wet wick, is exposed to air passing over it. The wick and therefore the thermometer bulb decreases in temperature below the dry-bulb temperature until the rate of heat transfer from the warmer air to the wick is just equal to the rate of heat transfer needed to provide for evaporation of water from the wick into the air stream.

Equating these two rates of heat transfer gives

$$\alpha A(t - t_w) = h_{fg}\beta(H_s - H_a) \tag{2.7}$$

Where α and β are the heat transfer coefficient and mass transfer coefficient respectively; t and t_w are dry-bulb and wet-bulb temperature respectively; H_s and H_a are the specific humidities of saturated air and dry air and h_{fg} is the latent heat of evaporation of water.

As the relative humidity of the air decreases, the difference between the wet-bulb and dry-bulb temperatures, called the wet-bulb depression, increases and a line connecting wet-bulb temperature and relative humidity can be plotted on a suitable chart. When the air is saturated, the wet-bulb temperature and the dry-bulb temperature are identical.

Therefore if $(t - t_w)$ is plotted against $(H_s\text{-}H_a)$ remembering that the point (t_s, H_s) must correspond to a dew-point condition, we then have a wet-bulb straight line on a temperature/humidity chart sloping down from the point (t_s, H_s) with a slope of $-(h_{fg}\beta/\alpha)$.

A further important concept is that of the adiabatic saturation condition. This is the situation reached by a stream of water, in contact with the humid air, both of which ultimately reach a temperature at which the heat lost by the humid air on cooling is equal to the heat of evaporation of the water leaving the stream of water by evaporation.

Under this condition with no heat exchange to the surroundings, the total enthalpy change

$$\Delta H = c_s(t - t_s) + \beta(H_s - H_a) = 0 \tag{2.8}$$

Where c_s is the humid heat of the air.

Now it just so happens, for water, that the numerical magnitude of the Lewis number, Le, is

$$Le = \frac{\alpha}{c_s \beta} = 1$$

Therefore the wet bulb line and adiabatic saturation line coincide when the Lewis number equals to 1.

Now is the time to talk about the psychrometric chart. In the preceding discussion, a chart of humidity against temperature has been considered. Such a chart called psychrometric chart is shown as Appendix II. The two main axes are temperature (dry bulb) and humidity. The saturation curve is plotted on this dividing the whole area into an unsaturated and a two-phase region. Taking a point on the saturation curve (t_s, H_s), a line can be drawn from this with a slope of ($-h_{fg}\beta/\alpha$) running down into the unsaturated region of the chart, this is the wet-bulb or adiabatic cooling line and a net of such lines is shown. Any constant temperature line between the saturation curve and zero humidity axis can be divided evenly into fractional humidity which will correspond to fractional relative humidity.

2.4 Convective Drying Models

To predict the performance of the dryers/separators, it is necessary to develop mathematical models to simulate the drying process in those dryers and predict the drying time.

Since the properties of the product particles are so different, it is almost impossible to establish a mathematical model that can cover all types of materials and dryers/separators. But from the performance of the dryers (Reference 23), it was found that the whole drying process could always be divided into two separate periods: The constant-rate and falling-rate periods. The drying rates when plotted as a function of solids moisture may describe a curve similar to the one in Figure 2.2. When the solids moisture decrease to the critical moisture content X_c, the drying rate is falling.

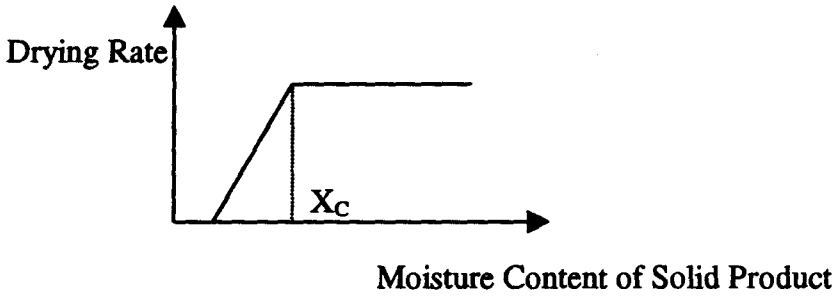

Figure 2.2 A typical drying curve

In his book on sanitary operations, Rich (1961) pointed out that for a lot of nonporous, granular particles, the curve during the falling-rate period may be approximated as a straight line, and drying will cease shortly after the plane where vaporization happens has passed through the product cake. He also pointed out that for porous and/or hygroscopic materials the drying curve could vary considerably from a

straight line during the falling-rate period. He provided a simple model based on the assumption that the drying curve would be a straight line during the falling-rate stage. (See Reference 5)

A lot of models of heat and mass transfer during convection drying of porous media have been set up recently.

Nasrallah and Perre (1988) deduced a model of heat and mass transfer in porous media. This model contained a very comprehensive set of equations and took into account the effect of gaseous pressure. They solved the equations numerically with unidirectional transfers. The evolution of temperature, moisture content and pressure as well as the overall drying kinetics were calculated for two different porous media. This device permitted one to study the sensitivity of the model to internal parameters and conditions at the interface as well as the effect of certain reductions in the model.

Sattler and Feindt (1994), in their book named "Thermal Separation Process", described a simple model of drying process between a saturated flat product bed and an external air flow along the bed. They pointed out that during the constant-rate stage, the drying rate is the same as the evaporation rate on the free water surface, but during the falling-rate stage, the drying will be controlled both by evaporation and vapor diffusion. But they did not tell what would happen when the air was purged across the product bed and how to determine the heat and mass transfer coefficients during the drying. They did not provide any information about Critical Moisture Content (CMC) of the product either.

To study the behavior of the heat and mass convective transfer coefficients at the interface between a porous media and an external flow air during the drying, Masmoudi

and Prat (1991) carried out numerical simulations of the drying process. They found that the interfacial transfer coefficient differ from the standard values corresponding to boundary layer flows on the flat plate with uniform temperature or concentration at the wall. They also studied the effects of the leading edge and occurrence of large-scale heterogeneities of water content at the interface during drying.

Oliveria et al. (1998) presented a methodology for the analysis of conjugate problems in the convective drying of porous media. They treated the interface between the porous medium and the external convective flow as an internal boundary within a two-phase system rather than a geometric limit. By expressing the continuity of the state variables and their respective fluxes through the interface, the problems of solid drying and convection boundary layer was connected. Wood-drying problems were also applied to evaluate this methodology. This analysis of the drying of porous media as a conjugate problem allows the assessment of the effect of the heat and mass transfer within the solid on the transfer in adjacent fluid, providing good insight on the complexity of the transfer mechanisms.

Recently, more and more researchers have concentrated their attention on the drying of porous media. Fernandez and Howell (1996) developed a transient one-dimensional model for the drying of a porous material (wood) that includes both heat and mass transfer. Heat transfer by conduction and convection, and mass transfer by binary gas diffusion, pressure-driven bulk flow in the gas and liquid, and diffusion of bound water are included in the analysis. The diffusive mass transfer terms are modeled using a Fickian approach, while the bulk flow is modeled assuming Darcian flow. Depending on the state of the moisture in the wood appropriate terms are considered in the development

of the governing mass equations. They provided the distributions with the material of each moisture phase (vapor, liquid, and bound), temperature and pressure. The information of drying rate and evaporation rate was also presented and compared with experimental data.

Wang and Fu (1995) set up a simplified model of heat and mass transfer during the convective drying of banana pieces. Capillary action zone, vapor diffusion zone and transition zone were described in one diffusion equation and a theoretical expression of the effective diffusivity is obtained by taking account the transfer mechanisms of capillary action and vapor diffusion. The model was solved numerically and the calculation procedure proves very simple. The predicted values were found to meet the experimental data very well.

Murugesan et al. (1996) applied a one-dimensional finite element analysis to study temperature and moisture variation of porous materials during convective drying. They used Henderson's modified equation to obtain the desorption data for the materials and the predicted results for brick and mortar with constant transport properties agree with available experimental data.

Sun and Marrero (1996) presented results of theoretical and experimental studies on heat and moisture transfer around single short porous cylinders during forced convective drying. Air was passed across saturated coal logs, varying air humidity, temperature and velocity, as well as log aspect ratio and diameter. After considering the transport coupling effects, the coupled heat and mass transfer results are correlated in terms of the dimensionless Nusselt and Sherwood numbers. The surface temperatures during drying

were well estimated using a modified energy balance formula. Their correlation is useful to predict the initial drying rate for short cylinders with an aspect ratio from 1.2 to 2.0.

Based on classifying analysis and conclusive comments about various kinds of drying model, Zhang and Yang (1997) established a relative comprehensive model to describe heat and mass transfer during constant rate and falling rate periods in convective drying of porous media. They introduced the concept of iterative correction and corresponding numerical method was developed for moving boundary problem in numerical simulation of drying process. Their calculation results for drying of bricks was said to be more precise than other models.

From preceding discussions, it seems difficult to establish a comprehensive model that is suitable for all kinds of materials and for all types of drying manners. The reason is that with different materials and drying manners, the mass and heat transfer behaviors are different. Some models are accurate but they will cost too much calculation time, which is not suitable in practical applications. In this research thesis, the goal is to establish a simple but reliable mathematical model for a vacuum separator.

Chapter 3 Mathematical Modeling

3.1 Introduction

In this chapter, a mathematical model is developed to predict the drying time for a slurry product suspended above a metal screen through which air is passed. This model has application to the drying of pharmaceutical and other particle slurries.

The configuration of the model is shown in Figure 3.1. By vibration, wet particles are suspended above the screen. Air passes through the product cake, picks up moisture and dries the product particles.

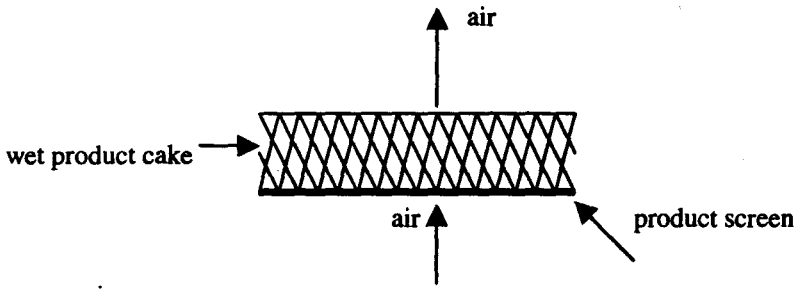

Figure 3.1: Geometry of the product

3.2 Process description and assumptions

The wet product is a kind of porous material that is saturated with water and it is obvious that the actual heat and mass flow picture inside the product is complicated. The flow geometry differs unpredictably from one region of the product to another. To simplify the problem, it is necessary to eliminate the local complication and unpredictability of the heat/mass transfer phenomenon. A common simplification is to assume the wet product cake contains a certain small-scale network of channels of known geometry and the air would flow through each channel.

An applicable assumption is that there is bundle of capillary tubes inside the product cake. Air is purged across the product cake through these capillary tubes, around these tubes is the wet solid product. The geometry of capillary tubes, airflow and wet solid product could be shown in Figure 3.2.

During the drying process, heat is transferred from the drying air to the wet solid product and is used to evaporate residual liquid from the product into the air.

To evaporate moisture from the product into the air, the temperature of the product will decrease so that heat can be transferred from the drying air to the wet product. If the product is wet enough, the temperature will decrease to a certain value at which the heat transferred from the air will be equal to the latent energy supplied for the evaporation; this temperature is the wet-bulb temperature of the air. During the drying process, the temperature of the product will be maintained at the wet-bulb temperature for a long time.

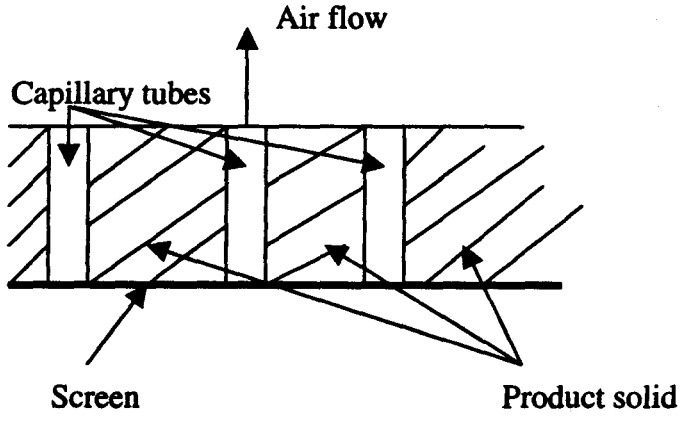

Figure 3.2 Geometry of Drying Interface

As mentioned in Chapter 2, there are three main kinds of moisture existing in the wet product: adsorbed liquid, capillary liquid and swelling liquid. If the adsorbed liquid is evaporated out, the capillary forces that deliver the moisture to the drying front will control the moisture flow inside the product slurry. The drying front could be defined as the surface where the moisture exists in the form of liquid. It is an important concept of this model.

Another concept introduced is the effective length of the capillary channels. The dry air is cooled and wetted through the capillary channels by the heat/mass transfer. Air temperature and humidity will change along these channels. To simplify the problem, the total length of the capillary tube is divided into two parts. In the beginning part of the tube, air is assumed to have the same temperature and humidity as the inlet purging air and the length of this part is defined as the "effective length". Heat and mass transfer happen and the drying is effective. In the rest of the tube, the air is assumed saturated and no drying will happen at all.

The effective length is greatly influenced by the air-bleeding rate. If the air-bleeding rate is large enough, the cooled and wetted air will be purged out of the capillary channels immediately. The whole channel is filled with dry, fresh air and the effective length can be the whole length of the channel.

The effective length is also influenced by the drying rate between the air-solid interface. If the drying rate is larger, it is easier to saturate the air and the effective length should be shorter.

Other assumptions also include:

1. There are no heat transfer between the product and the environment during the drying process; the heat carried away by the evaporated moisture is equal to the heat supplied to the process by the drying air. This balance between the supplied and withdrawn heat at the drying front of the product controls the course of the drying.
2. The drying phase is water.
3. The temperature of the drying front is the wet-bulb temperature.
4. The properties of the product such as density and thermal conductivity are constant throughout the cake.
5. The air can only go through the capillary channels, around the channels is the wet solid products that is made up of solid particles and moist liquid.

3.3 Model Development

During the early stage of the process, the temperature of the product will decrease. A negligible amount of moisture is evaporated during this short period, then the main drying process begins. It can be divided into two stages.

In the first drying time, the product is wet enough, so that the drying front is the interface between the purging air and the solid products (shown as Figure 3.3). Since the amount of moisture evaporated is delivered from the inside of solid products to the drying front by capillary forces, the product surface behaves like a free liquid surface with respect to evaporation. Therefore, the drying rate is the evaporation rate of moisture from the air-solid interface. The drying rate is thus a function of the mass transfer coefficient and the difference between the wet air-solid interface humidity H_s, and bulk air humidity

H_a. The type of moisture and the condition of the air bleeding will also affect the drying air.

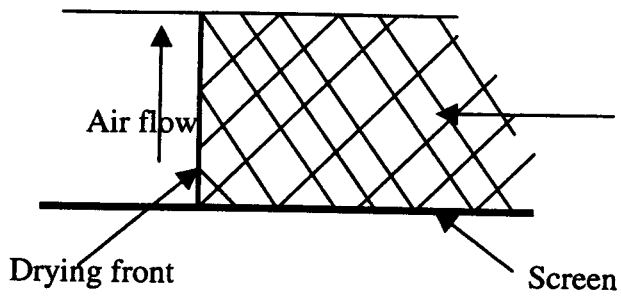

Figure 3.4 Drying front of constant stage

The amount of moisture evaporated per unit time is:

$$\dot{m} = \beta A \rho (H_s - H_a) \tag{3.1}$$

The energy balance should be:

$$\dot{Q} = \alpha A (t - t_w) \tag{3.2}$$

Since there is no heat loss during the process:

$$\dot{Q} = \dot{m} h_{fg} \tag{3.3}$$

The heat transfer coefficient is much easier to obtain than the mass transfer coefficient. Therefore Equations (3.1) (3.2) (3.3) can be rearranged to obtain:

$$\dot{m} = \frac{\alpha}{h_{fg}} A(t - t_w) \tag{3.4}$$

Where α is the heat transfer coefficient between the purging air and the solid product. The area for the heat/mass transfer should be the total aspect area of the capillary channels.

Equation (3.4) demonstrates that for drying air with given conditions (temperature, humidity, pressure, and velocity), the drying rate is constant. With this constant drying rate, the moisture content of the product decreases.

When the moisture content of the product decreases to a certain value, the rate at which moisture delivered to the drying front by capillary action is less than the evaporation rate, and the drying rate decreases. The moisture content when this begins is called critical moisture content.

The drying front moves away from the surface to the inside of the product (shown in Figure 3.4). The drying rate is now controlled by the heat conduction at the dry product surface, by the capillary moisture conducted from inside the product to the drying front, by moisture diffusion from the drying front to the product surface, and by transfer of the evaporated moisture into the air. As the drying front moves away from the product surface, the drying rate decreases with time. This occurs because the conduction resistance and diffusion resistance in the second drying stage is increasing.

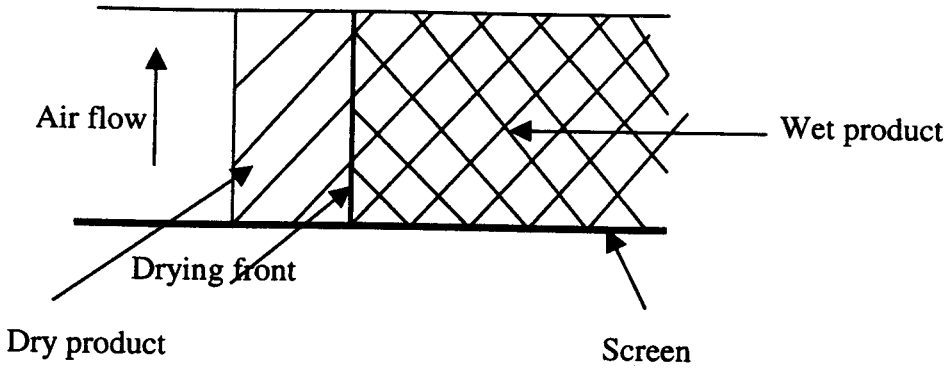

Figure 3.4 Geometry of drying on decreasing-rate stage

In this case, the evaporated moisture rate is:

$$\dot{m} = (H_s - H_a)A\rho/(1/\beta + s/D) \tag{3.5}$$

The energy balance should be:

$$\dot{Q} = \frac{(t - t_s)A}{(1/\alpha + s/k)} \tag{3.6}$$

So, from (3.3):

$$\dot{m} = \frac{\frac{(t - t_s)A}{(1/\alpha + s/k)}}{h_{fg}}$$

(3.7)

From Equation (3.7), it is seen that the drying rate decreases with time.

If the drying continues, the drying front will eventually disappear. That is to say there no longer be any liquid. For nonhygroscopic materials, the product is considered to be dry at this point. For hygroscopic materials, the drying may need to continue. But at this point, diffusion controls the drying process and drying rate, which is still decreasing, is very low. The temperature of the product will increase slowly until it is the same as the purging air. Since in this stage, the drying rate is very slow and has little influence in the total drying time prediction. In this model, this stage will not be considered.

Now, the required drying time to dry a product could be calculated, because:

$$\frac{dX}{d\tau} = \frac{\dot{m}}{G}$$

(3.8)

Suppose the moisture content of the product decreases from X_B to X_D throughout the drying process. X_C is critical moisture content which divides the whole process in two parts, so:

$$\tau = G\int_{X_B}^{X_D} \frac{dX}{\dot{m}}$$

(3.9)

The whole drying time τ can be calculated like this:

$$\tau \approx G\left(\int_{X_C}^{X_B} \frac{dX}{\dot{m}_{BC}} + \int_{X_D}^{X_C} \frac{dX}{\dot{m}_{CD}} \right) \tag{3.10}$$

Since drying rate is constant during process BC,

$$\tau \approx G\frac{(X_B - X_C)}{\dot{m}_{BC}} + G\int_{X_D}^{X_C} \frac{dX}{\dot{m}_{CD}} \tag{3.11}$$

This is the formula we use to calculate the whole drying time of the separator.

3.4 Parameters Determination

From the preceding analysis, if we use Equation (3.4) and (3.7) to calculate drying rate, or use Equation (3.10) to calculate the total drying time, it is necessary to have access to the following parameters: heat transfer coefficient, wet-bulb temperature, the mass/heat transfer area, and critical moisture content.

3.4.1 Heat transfer coefficient

The best way to access the heat transfer coefficient is by experiments. Rich (1961), in his book "Unit Operation in Sanitary Engineering", suggested the following Equations:

When air flow is parallel to the drying plane, it has been found that

$$\alpha = 0.0128 G_G^{0.8} \tag{3.12}$$

For air flow normal to the drying plane,

$$\alpha = 0.37 G_G^{0.37} \tag{3.13}$$

Where G_G = mass velocity of dry air, kg/(m^2)(hr)

Rowe et al. (See Reference 2) reported that for particles suspended in the air flow, it was found that:

$$\alpha = \frac{\lambda}{d}\left[2 + 0.54\left(\frac{d\,u}{\nu}\right)^{0.5}\right] \tag{3.14}$$

Equation (3.14) is suitable for the case where the air bleeding rate is very high, especially for the fluidized product bed.

To better study the variation of heat and mass transfer coefficients during drying of granular beds, Rogers and Kaviany (1988) measured the evaporation rate from a granular bed using various particle sizes. With an estimate of the liquid and solid surface area (using the Young-Laplace formulation) for the large diameter particles, they use the experimental results of evaporation rate to determine the heat and mass transfer coefficients.

3.4.2 Determination of the wet-bulb temperature

The easiest way to obtain the wet-bulb temperature is to use a computer program, which interpolate from a psychhromarics chart.

For the wet air, its entropy can be expressed as:

$$i = i_a + \omega \cdot i_m \qquad (3.15)$$

where i_a is the entropy of the dry air (kJ/kg dry air)

ω is the absolute humidity of the air (kg moisture/kg dry air)

i_m is the enthalpy of the moisture (kJ/kg moisture)

and

$$i_a = c_{p,air} \cdot t$$

$$i_m = 2500 + c_{p,moisture} \cdot t$$

Where $c_{p,air}$ is specific heat of the air at constant pressure(about 1.005 kJ/kg°C)

$c_{p,moisture}$ is specific heat of the vapor at constant pressure (about 1.84 kJ/kg°C)

2500 is the latent heat of the water at 0°C (kJ/kg)

Introducing the values of specific heat into Equation (3.15):

$$i = 1.005t + \omega(2500 + 1.84t) \qquad (3.16)$$

And absolute humidity is given by Equation (2.4):

$$\omega = 0.622 \frac{p_v}{p - p_v}$$

The partial pressure of the vapor p_v can be expressed as:

$$p_v = \phi p_s \tag{3.17}$$

Where p_s is partial pressure of the vapor in the saturated air

ϕ is relative humidity of the air

Introduce Equation (3.16) and (3.17) into Equation (3.15):

$$i = 1.005t + o.622 \frac{\phi p_s}{p - \phi p_s} (2500 + 1.84t) \tag{3.18}$$

Since the drying process is adiabatic,

$$i_t = i_{t_w} \tag{3.19}$$

When air enters the separator, p = 1 bar and when temperature decreases to the wet-bulb temperature, φ = 100% = 1. Introducing them into Equation (3.18):

$$i_t = i_{t_w} = 1.005t_w + 0.622\frac{p_{s,(t_w)}}{p - p_{s,(t_w)}}(2500 + 1.84t_w)$$
$$= 1.005t + 0.622\frac{\phi p_{s,t}}{1 - \phi p_{s,t}}(2500 + 1.84t) \qquad (3.20)$$

With given temperature and humidity of the air, the corresponding wet-bulb temperature can be determined by Equation (3.20). The partial pressure of the vapor in the saturated air can be found in Appendix I. A small program provided in Appendix II also determines the wet-bulb temperature with Equation (3.20).

3.4.3 Estimation of the Heat/Mass Transfer Area

The heat/mass transfer area can be estimated as following:

$$A = N\pi d_c l_e \qquad (3.21)$$

Where N is total number of the capillary channels, d_c is the mean diameter of the capillary channels, and l_e, is the effective length.

The effective length is constant during the constant-rate stage. During the falling-rate stage, the effective length will be larger and larger until it occupies almost the whole length of the channel with a falling drying rate.

The diameters of the channels should be much larger than that of the particles, or the channel can be blocked by the vibrating particles and thus be destroyed. I supposed that the mean diameter of the channels is about ten times of the mean size of the particles.

The total number of the channels can be estimated with the screen area and the diameter of the capillary channels.

3.4.4 Critical Moisture Content

The critical moisture content is normally determined experimentally, since it is difficult to predict mathematically. The following factors influence it: thickness of the product cake, air bleeding rate, humidity and temperature, and the chemical and physical properties of the product particles. It will be discussed in details in Chapter 6.

3.5 Mathematical Algorithm and Results

With Equation (3.7) and (3.10), the drying rate and the total drying time can be calculated. It should be pointed out that s, the distance from the drying front to the air-solid interface, is changeable.

To solve the problem, Equation (3.7) should be discretized as:

$$m_i = \frac{(t - t_w)A}{h_{fg}(1/\alpha + s_i/k)} \qquad i = 1,2,3,\cdots,n. \tag{3.22}$$

where $s_n = l$

And Equation (3.10) can be changed into:

$$\tau = G\frac{(X_B - X_C)}{m_{BC}} + G\sum_{i=1}^{n}\frac{(X_C - X_D)}{nm_i} \tag{3.23}$$

A small program based on Equations (3.22) and (3.23) is provided in Appendix II.

Figure 3.5 shows the variation of the drying rates of a separator operated under three different vacuum levels. (Other conditions are the same: 12 inch-diameter screen, inlet air with 30% humidity and 20°C, product particles are glass beads with critical moisture content of 0.2 and initial moisture content of 0.5, total dry product is 1 kg.)

It is obvious that all the curves can be divided into two stages: Constant-rate stage and decreasing-rate stage, and with a better vacuum level, the drying rate is higher.

Figure 3.6 shows the drying curves with different inlet air temperature. Drying will be faster with a higher inlet air temperature since warmer air has the ability to pick up more moisture.

Figure 3.5: Drying rate curve under different vacuum levels

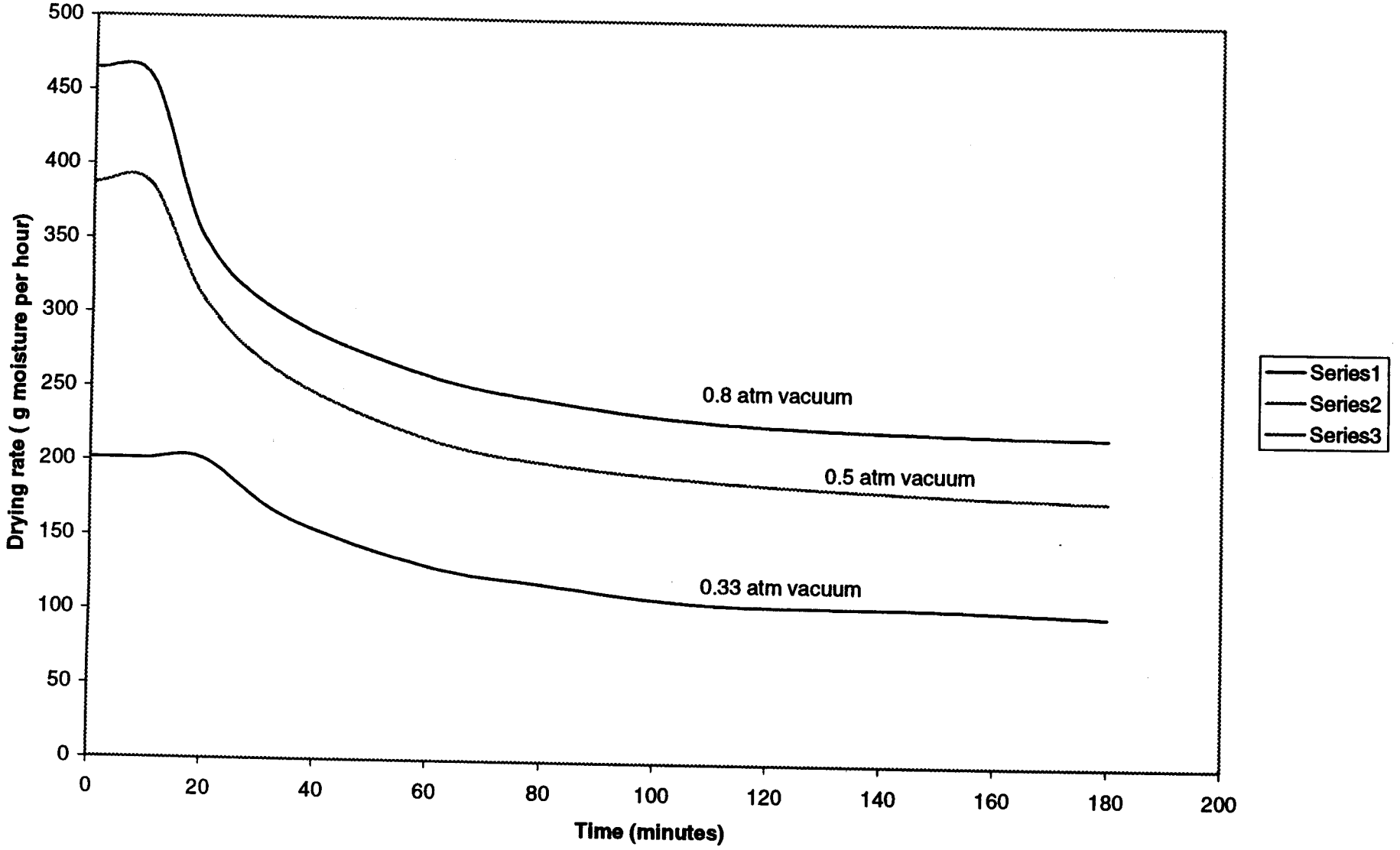

Figure 3.6: Drying rate curves with different inlet air temperature

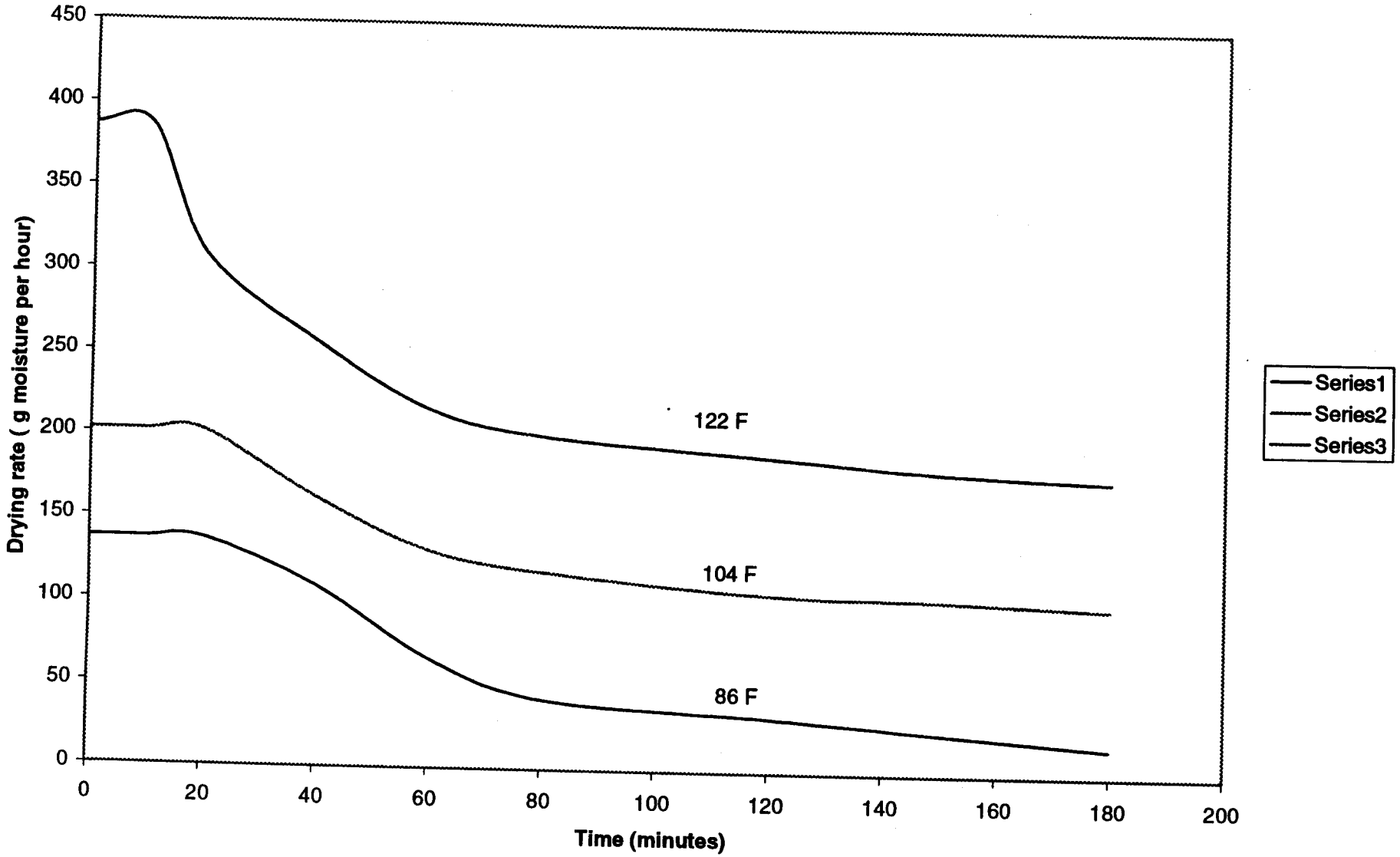

Chapter 4 Experimental design and procedure

In this chapter, the apparatus and measurements procedure will be discussed.

4.1 Goals

The primary goal of these experiments is to measure the drying rate and compare it with the mathematical model.

So, first, it is necessary to study the variation of moisture content of the product throughout the drying process; secondly, the variation of the air humidity at the inlet and exit need to be investigated.

The factors, which affect the drying rate, should also be investigated.

4.2 Apparatus

A schematic of the apparatus is shown in Figure 4.1. Air was drawn across the product cake through a product screen. Twenty-five percent of this screen area is open area including holes with diameters of approximately 10 microns. The air was heated using an air-blower-heat exchanger placed at the entrance to the air channel. Temperature probes were installed at the entrance and exit of the air channel and vacuum was pulled through the top of the separator. The three openings on the separator cover were used as the feeding post, sight glass and for plug assembly used to check the product particles.

An air humidity probe (Vaisala HMP-235) was installed a half inch above the product cake to measure the exit air humidity and temperature. Air bleeding rate and vacuum level could be read directly from the flow meters and vacuum gauge, respectively.

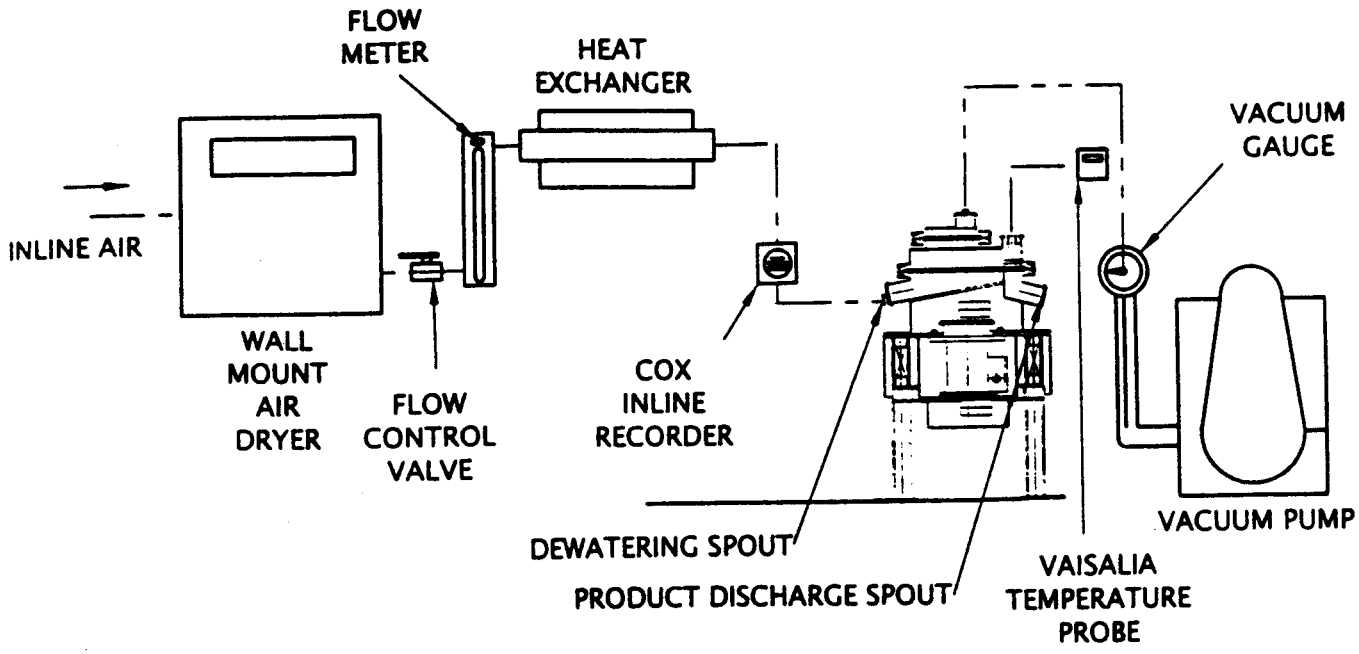

Figure 4.1 A schematic of the apparatus

A Vibro-Separator/vacuum dryer combination, the PharmASep developed by SWECO Company is designed specifically for the pharmaceutical industry. It has the ability to dewater the slurry on the screen, apply vacuum, dry the product and discharge the dried product. Experiments were performed using three different models of PharmASep, 12 inches, 18 inches and 30 inches (screen diameter).

In these experiments, it is not convenient to insert a wet-bulb thermometer for measuring humidity. Therefore, capacitance humidity sensors were used.

4.3 Measurement

During a normal experimental run, the following procedures were followed:

- The moisture content of the product particles were measured at approximately ten minutes intervals.
- The entering and exiting air temperature, humidity and flow rate were measured.

• The critical moisture content was investigated.

The product particles (glass beads, around 50 μm in diameter) were initially suspended in a 0.5% slurry. Slurry was introduced through a feeding port while the unit was vibrating and the free water was discharged through a water-discharge port. The discharged water was weighed to calculate the wet slurry cumulated on the separator screen.

Then the drying process began. The pre-heated purging air, and the vacuum pump were turned on and adjusted so that the air bleeding rate, vacuum level and temperature of the purging air could be kept constant throughout the drying process.

Every five minutes, the temperature and humidity of the purging air and the exiting air were measured. The product samples (less than 0.5% of total wet product weight) were drawn from the product screen either throughout the drying cycle, or at completion of the test.

The exit air was and remained saturated for the first few hours of the drying cycle. At the point of rapid and considerable fall in humidity of the exiting air, the moisture content of the product should be the critical moisture content.

The moisture content of the product samples was usually evaluated either by a micro-balance/heater system (Metler HG 53 moisture analyzer), or, by TGA (Thermal Gravimetric Analyzer). The drying cycle was assumed to be completed when the moisture content of the product was below 0.5%.

Tests were performed using different size separators, i.e. 12 inches and 30 inches units, or under different conditions (vacuum level, purging air flow rate, temperature, humidity etc.).

The heater exchanger was used to control the temperature of the bleeding air and the line air was dried with a wall-mounted dryer set. A controlled vacuum was pulled from the top (feeding port) of the separator using a vain pump (low level vacuum) or Stokes dry pump (high level vacuum).

Chapter 5 Results

In this chapter, experimental results obtained by the procedures described in Chapter 4 are plotted, discussed and compared with mathematical results based on the theoretical model developed in Chapter 3.

5.1.1 Variation of product moisture content

With a 30" PharmASep, under three different levels of vacuum and air bleeding rates, the variation of moisture content of the product particles throughout the drying process is tabulated in Table 5.1 and plotted in Figure 5.1:

Time (hour)	Moisture(%) (4 scfm/ 20" Hg)	Moisture(%) (10 scfm/14" Hg)	Moisture (%) (17 scfm/5" Hg)
0	20	20.7	21.4
0.2	18.5	18.1	18.1
0.5	18.2	17.5	17.6
1.5	18.1	16.4	16.2
2	17.5	14.3	13
2.5	16.9	12.3	10.7
3.5	13.6	8.4	7.5
4.5	12.1	6.1	5.1

Table 5.1 Variation of moisture content of product during the drying process

In Table 5.1 and Figure 5.1, the indicated "Hg is the vacuum level. (For example, 20 inches Hg vacuum equals 9 inches Hg absolute pressure)

Both the air bleeding rate and vacuum level are important factors influencing the drying rate. As we may conclude from theoretical and experimental evidences, the larger

the air bleeding rate, the higher the drying rate. And also, the better the vacuum level the faster the drying process.

From Table 5.1 and Figure 5.1, it is obvious that with a large air bleeding rate but a poor vacuum level, the drying rate is higher than that with a small air bleeding rate but a good vacuum level. It seems that the air-bleeding rate plays a more important role than the vacuum level. The reason is that a large air-bleeding rate can greatly increase the effective length of the capillary channels inside the product cake and thus will increase the effective heat/mass transfer area and drying rate. If a higher vacuum level but a lower air-bleeding rate is introduced, even though the drying rate per unit area will be increased, the effective length and thus the effective heat/mass area will be smaller and the drying rate is lower.

Another reason is that for a good vacuum level, the temperature of the product and the exit air should decrease greatly, but due to the heat transferred from the environment, the exit air and product temperature could not decrease as low as predicted. Therefore the drying rate could not be increased as greatly as predicted.

5.1.2 Variation of exit air humidity

Glass beads were dried on the screen of a PharmASep 12" under the following conditions: 70°F purging air temperature, 2 scfm bleeding air flow rate, 0% purging air humidity, 8-10" Hg of vacuum. The exit air humidity and temperature were measured as described in Chapter 4. The exit air temperature and humidity throughout the drying process can be plotted as in Figure 5.2.

Figure 5.1: Variation of the moisture content of the particles throughout the drying time

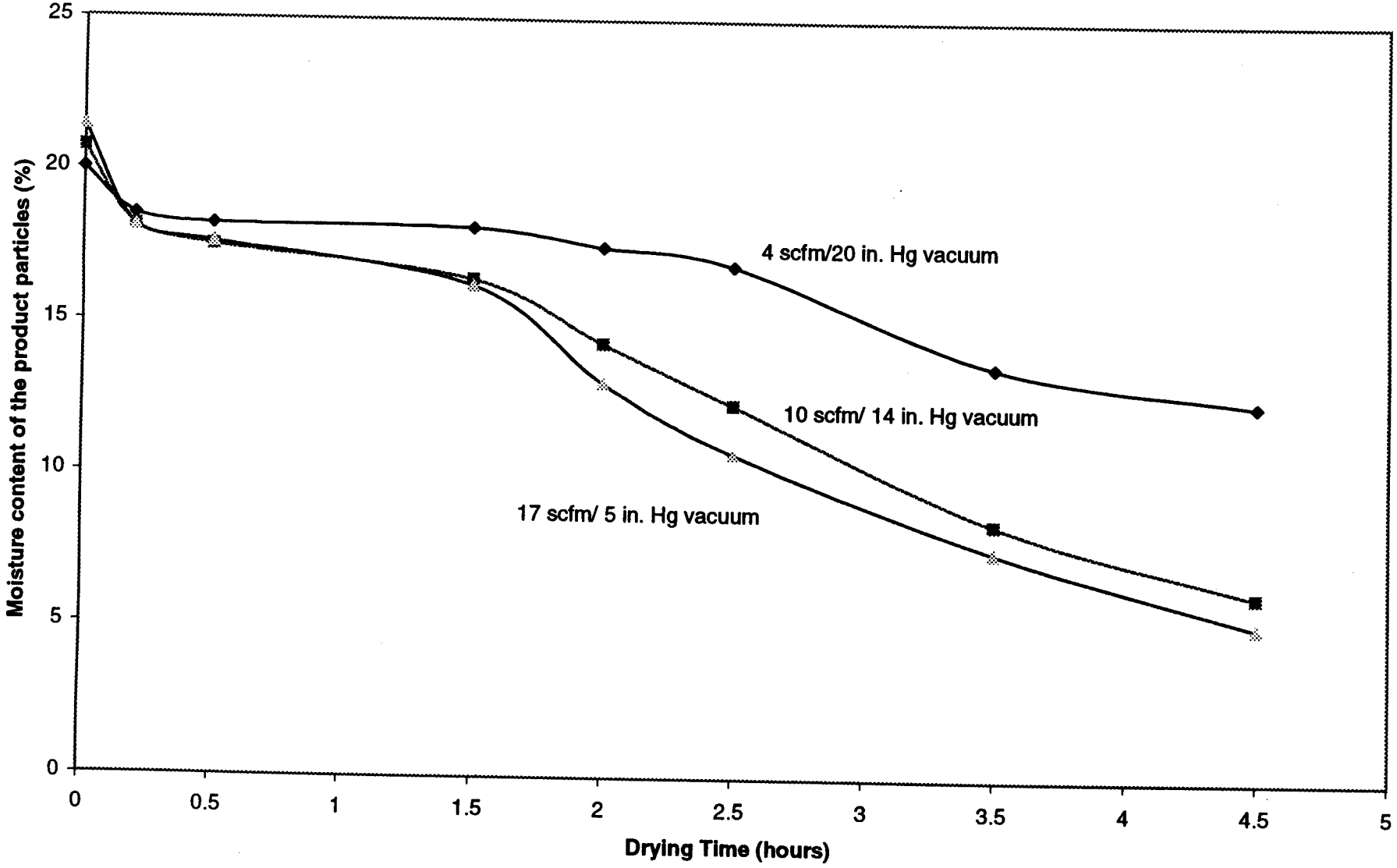

Figure 5.2: Variation of relative humidity and temperature of exit air

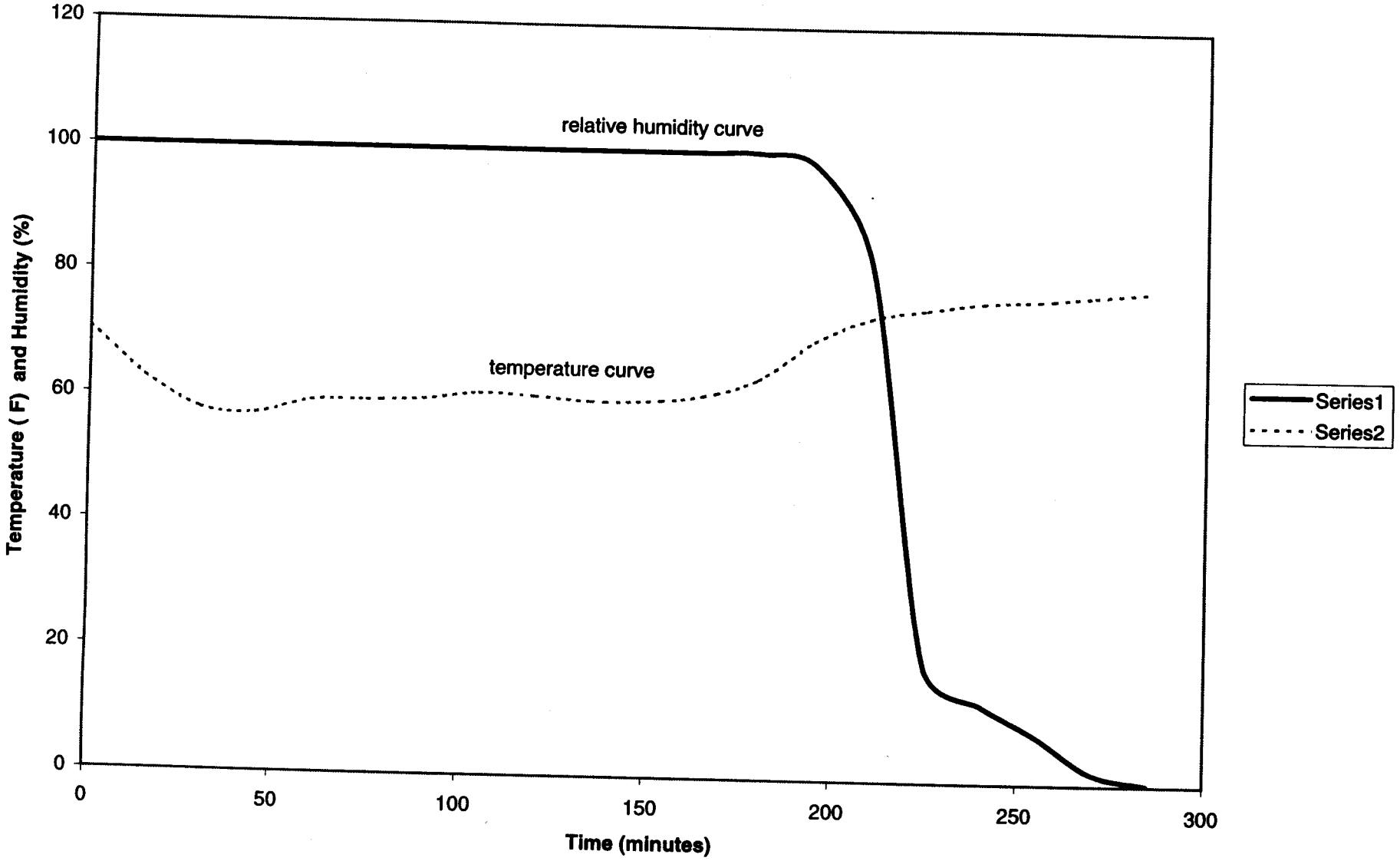

At the beginning of drying, the exit air humidity quickly reaches to nearly 100%, this saturated state may last for several hours. This period can be regarded as the "constant rate stage". Then the exit humidity decreases sharply, this means the drying rate is also decreasing, this is the "decreasing rate stage". At the end, where the exit air humidity changes slightly and eventually plateaus, drying has stopped.

The exit air temperature decreases in the initial stage of the drying process, then remains constant at 58°F throughout the "constant rate stage". When the humidity of the exiting air decreases, the temperature of the air increases, and remains constant at the latter part of the drying cycle. It is noticed that during the "constant rate stage", the exit air temperature remains at about 58°F. This temperature is different from the corresponding wet-bulb temperature (≅44°F). The reason is that there is heat generation due to the vibration of the screen and product. The total energy generated can be given by:

$$E = L(h_{t_{actual}} - h_{t_w}) \tag{5.1}$$

Where $h_{tactual}$ and h_{tw} are the enthalpy of saturated air at the actual exit air temperature and the wet-bulb temperature, respectively.

For the case in Figure 5.2, introducing the values of the corresponding parameters into Equation (5.1), the total energy generated by vibration is about 28 Watts. If the output of a vibrating device is 1000 Watts, that means 2.8% of its output cause the increase of the exit air temperature.

Heat may also be transferred from the environment to the whole drying system.

Figure 5.3 and 5.4 show the variation of exit air humidity and temperature with varying inlet air temperature, respectively. From Figure 5.3, it is obvious that with a higher inlet air temperature, the constant stage will be shorter; and From Figure 5.4, it can be seen that with a higher inlet air temperature, the exit air temperature would be higher.

5.1.3 Experimental drying rate

With the parameters of the inlet and exit air (humidity, temperature and bleeding rate), the transient-drying rate can be calculated. This rate can be considered as the experimental drying rate. The transient drying rates curve corresponding to Figure 5.2 is plotted in Figure 5.5. It is obvious that this curve can be divided into two stages: "constant stage" and "decreasing stage". It is interesting that there are two bumps in this curve. In the very beginning of the drying, since exit air temperature is decreasing while the air is still saturated, the drying rate is decreasing until the energy equilibrium is reached. This is a very short stage. Then the real constant stage begins and product becomes drier and drier. When the moisture content of the product decreases to the critical moisture content, the moisture that is transported to the air-solid interface is not fully evaporated. Exit air temperature will increase while the air is still saturated. The corresponding drying rate is also increased during this period. But this saturation cannot last long since the drying front retreats and moves toward the inside of the solid product and diffusion begins to influence the drying process. Exit air humidity and drying rate decreases at this time.

The drying rate curve corresponding to Figure 5.3 and 5.4 is plotted in Figure 5.6. The drying rate increases with a higher inlet air temperature.

Figure 5.3 Experimental exit air humidity curves as a function of inlet air temperature

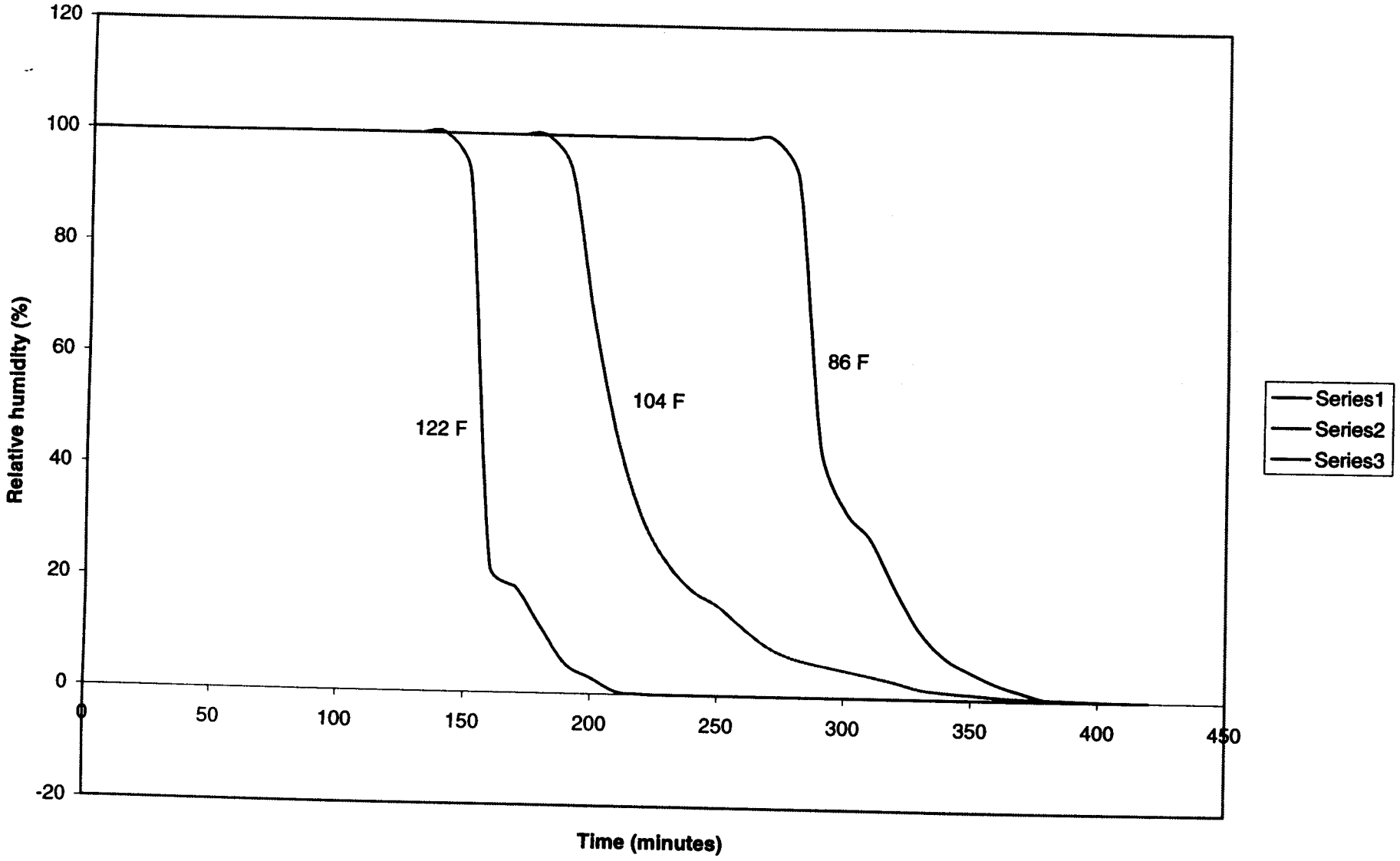

Figure 5.4: Experimental exit air temperatures as a function of inlet air temperatures

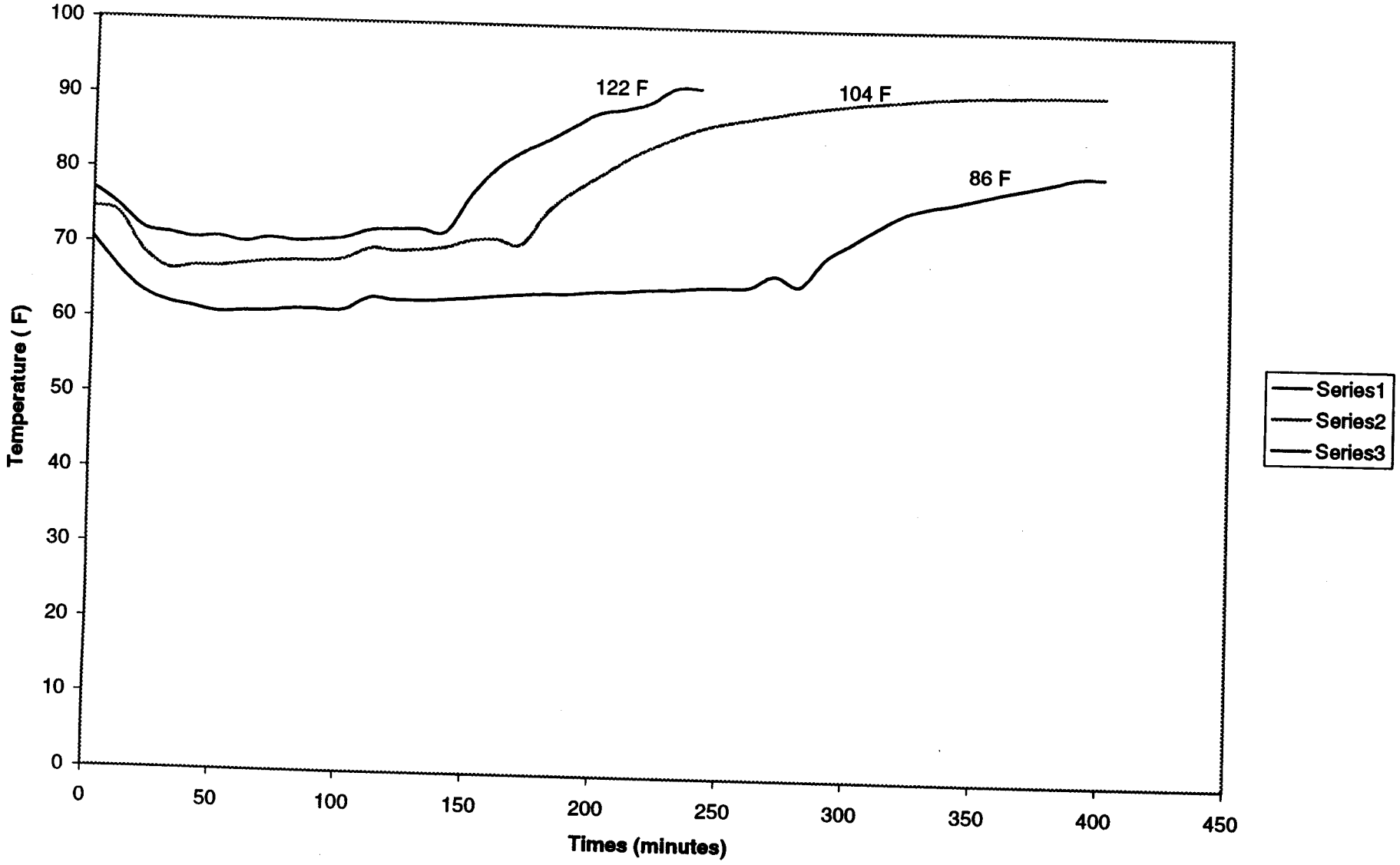

Figure 5.5: A experimental drying rate curve

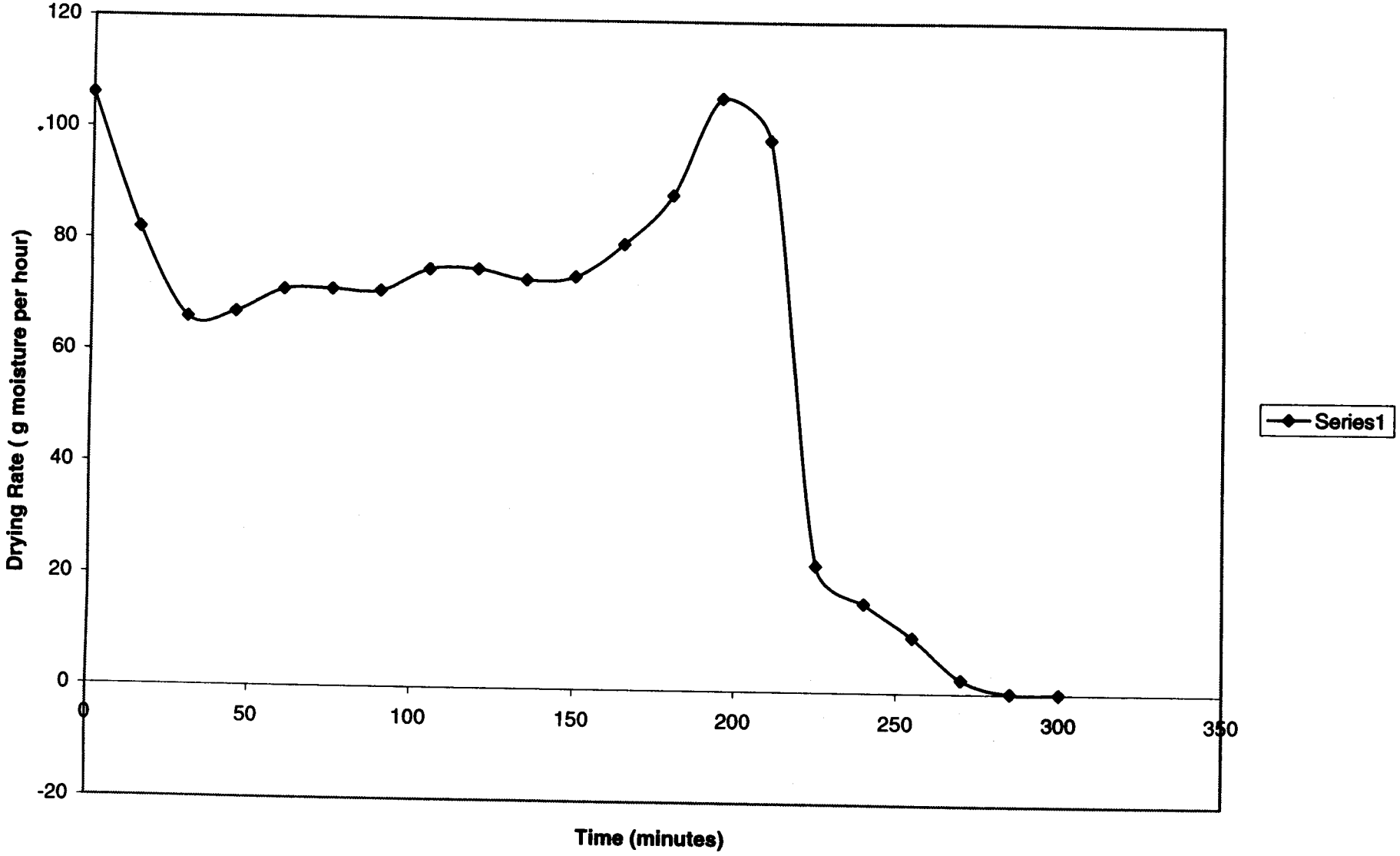

Figure 5.6: Experimental drying rate curves under different bleeding air temperatures

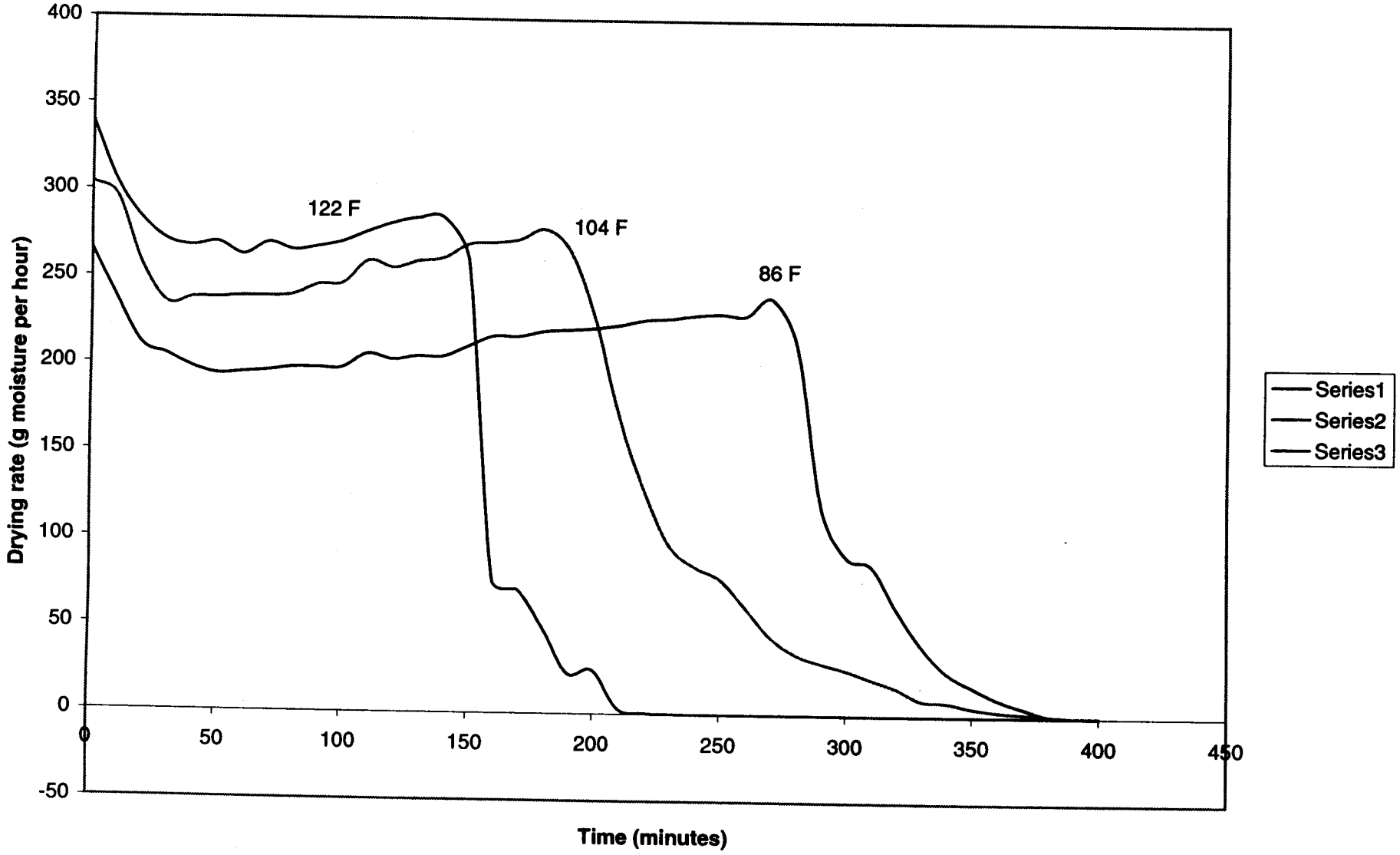

5.1.4 Uncertainty analysis

If a result R is a given function of the independent variables $x_1, x_2, \ldots, x_n$, thus:

$$R = R(x_1, x_2, x_3, \ldots, x_n) \tag{5.2}$$

Let w_R be the uncertainty in the result and $w_1, w_2, \ldots, w_n$ be the uncertainties in the independent variables. If the uncertainties in the independent variables are all given with the same odds, then the uncertainty in the result having these odds is given in Reference 3 as

$$w_R = \left[\left(\frac{\partial R}{\partial x_1} w_1\right)^2 + \left(\frac{\partial R}{\partial x_2} w_2\right)^2 + \ldots + \left(\frac{\partial R}{\partial x_n} w_n\right)^2\right]^{1/2} \tag{5.3}$$

The experimental drying rate was given by:

$$\dot{m} = L(\omega_2 - \omega_1) = 0.622L\left(\frac{\phi_2 P_{(t_2)}}{B_2 - \phi_2 P_{(t_2)}} - \frac{\phi_1 P_{(t_1)}}{B_1 - \phi_1 P_{(t_2)}}\right) \tag{5.4}$$

Where $P_{(t2)}$ and $P_{(t1)}$ are the partial pressure of the water vapor in the exit and inlet air, respectively. B_2 and B_1 are the total pressure of the exit and inlet air respectively, and normally, B_1 equals to one atmosphere.

To simplify the calculations, the critical moisture content of the product was assumed to be very small, thus the drying time could be given by:

$$\tau = \frac{GX}{\dot{m}} = \frac{GX}{0.622L\left(\frac{\phi_2 P_{(t_2)}}{B_2 - \phi_2 P_{(t_2)}} - \frac{\phi_1 P_{(t_1)}}{B_1 - \phi_1 P_{(t_1)}}\right)} \tag{5.5}$$

Where G is the total weight of the solid particles, X is the initial product moisture content.

Thus the uncertainty of the experimental drying time is given by:

$$w_\tau = \left[\left(w_{\tau(L)}\right)^2 + \left(w_{\tau(\phi_2)}\right)^2 + \left(w_{\tau(\phi_1)}\right)^2 + \left(w_{\tau(P_{i1})}\right)^2 + \left(w_{\tau(X)}\right)^2 + \left(w_{\tau(P_{i2})}\right)^2 + \left(w_{\tau(B_2)}\right)^2\right]^{1/2} \quad (5.5)$$

Where

$$w_{\tau(L)} = \frac{\partial \tau}{\partial \dot{m}} \frac{\partial \dot{m}}{\partial L} w_L$$

$$w_{\tau(\phi_2)} = \frac{\partial \tau}{\partial \dot{m}} \frac{\partial \dot{m}}{\partial \phi_2} w_{\phi_2}$$

$$w_{\tau(\phi_1)} = \frac{\partial \tau}{\partial \dot{m}} \frac{\partial \dot{m}}{\partial \phi_1} w_{\phi_1}$$

$$w_{\tau(P_{i1})} = \frac{\partial \tau}{\partial \dot{m}} \frac{\partial \dot{m}}{\partial P_{i_1}} w_{P_{i1}}$$

$$w_{\tau(P_{i2})} = \frac{\partial \tau}{\partial \dot{m}} \frac{\partial \dot{m}}{\partial P_{i_2}} w_{P_{i2}}$$

$$w_{\tau(X)} = \frac{\partial \tau}{\partial X} w_X$$

$$w_{\tau(B_2)} = \frac{\partial \tau}{\partial \dot{m}} \frac{\partial \dot{m}}{\partial B_2} w_{B_2}$$

The uncertainties of the partial pressure of the water vapor in inlet and exit air could obtain with the uncertainties of the inlet and exit air temperature.

A sample calculation is performed and results were tabulated in Table 5.2. Total solid particles weigh 1 Kg and total drying time is about 1.37 hour. Uncertainty of air bleeding rate is about 0.5 m^3/h, uncertainties of inlet and exit air humidity are 0.5% and 0% respectively. Uncertainties of partial vapor pressure could be obtained from the uncertainty of inlet and exit air temperature, which both are 0.01 bar. Compared with those of other variables, the uncertainty of the initial product moisture content is pretty large, which could be as large as 45%, and thus it will affect the final result greatly.

Parameters and Corresponding Uncertainties

L	t_2	t_1	ϕ_2	ϕ_1	B_2	X
8.5 m^3/h	20 °C	50 °C	100%	0%	0.5bar	60%
w_L	w_{Pt2}	w_{Pt1}	$w_{\phi 2}$	$w_{\phi 1}$	w_{B2}	w_X
0.5 m^3/h	0.01bar	0.01bar	0.5%	0%	0.066bar	45%
$w_{\tau(L)}$	$w_{\tau(Pt2)}$	$w_{\tau(Pt1)}$	$w_{\tau(\phi 2)}$	$w_{\tau(\phi 1)}$	$w_{\tau(B2)}$	$w_{\tau(X)}$
0.06 h	0.48 h	0.03h	0.03 h	0 h	0.13 h	1.02 h

Uncertainty of Drying Time

w_τ	τ	w_τ/τ
1.14 h	**1.37 h**	**83.2 %**

Table 5.2 A sample calculation of uncertainty of drying time

The uncertainty of total drying time could be as large as 1.14 hour and the relative uncertainty could be 83.2%.

In the next section, the uncertainty of the drying time could be compared with the errors between the mathematical predictions and experimental results.

5.2 Comparison between mathematical and experimental results

With above given experimental parameters, the model described in Chapter 3 can also simulate the whole drying process. The critical moisture content of the glass beads can be assumed or measured with the procedures described in Chapter 4. Since in the constant-rate stage the air-bleeding rate is normally not large enough to pick up moisture evaporated immediately, the drying rate was calculated with inlet and exit air parameters. The whole drying process is assumed to be adiabatic, the exit air could be saturated and its temperature is the wet-bulb temperature. The decreasing rate was calculated with Equation (3.7).

In Figure 5.7, the mathematical exit air temperature was compared with the experimentally measured air temperature at the exit, all the conditions are the same as those in Figure 5.2. The experimental temperature is about 15°F higher in the constant stage, but at the completion of the drying process, both temperatures are almost the same.

The exit air humidity was compared in Figure5.8. Both curves maintain 100% in the constant stage and then drop sharply. The experimental drying time is shorter than the mathematical prediction in the constant rate stage but in the decreasing-rate stage, experimental drying process is longer.

The experimental drying rate curve was compared with the mathematical drying rate in Figure 5.9. In the constant-rate stage, the actual drying rate was found to be much higher than mathematically predicted due to a higher exit air temperature.

At the completion of the drying process, the moisture content of the product can be considered as zero. With the transient experimental drying rate curve in Figure 5.9, the corresponding moisture content curve can be plotted in Figure 5.10 (the curve with

Figure 5.7: Comparison of exit air temperature curves

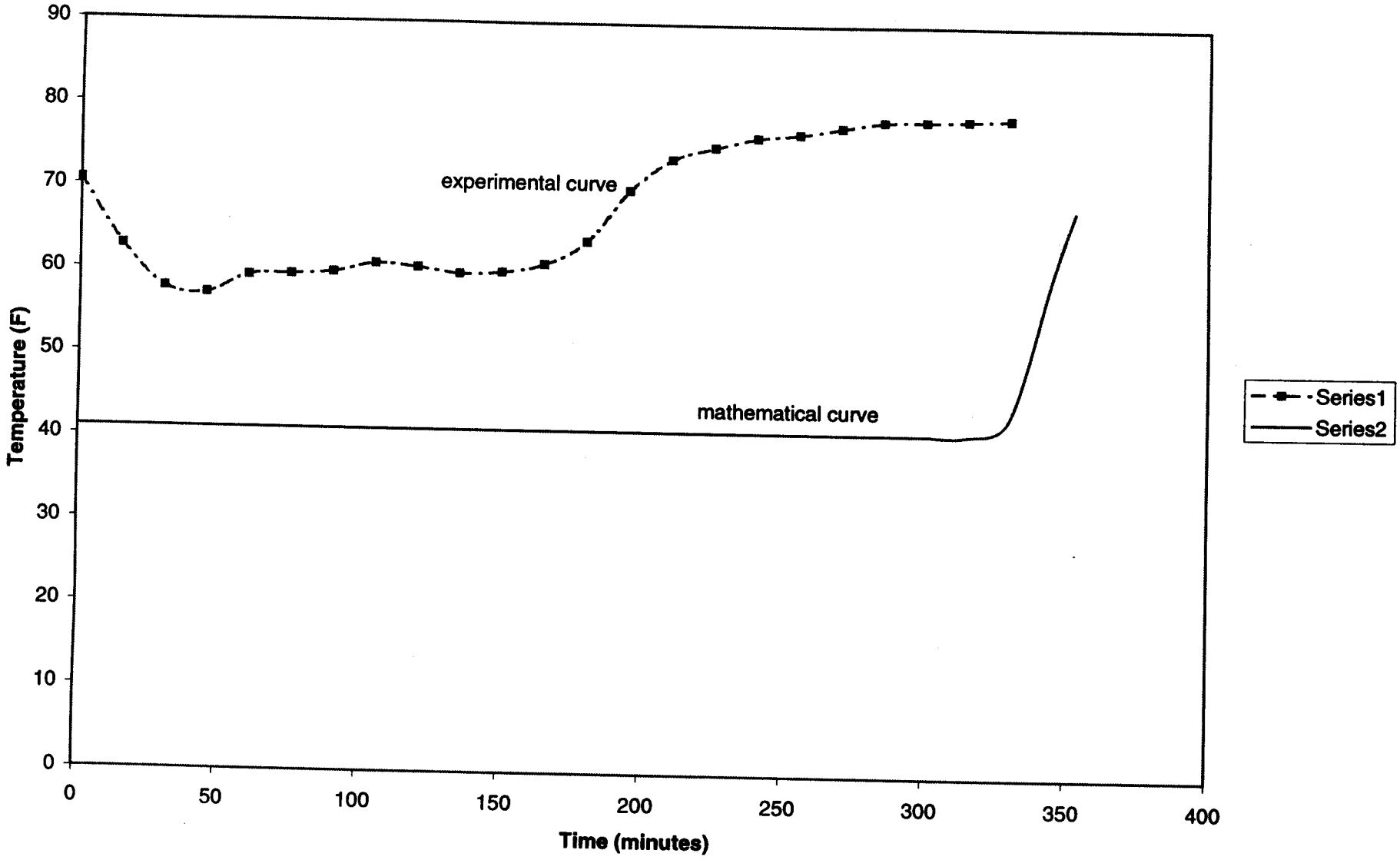

Figure 5.8 Comparsion between experimetal humidity curve and mathematical curve

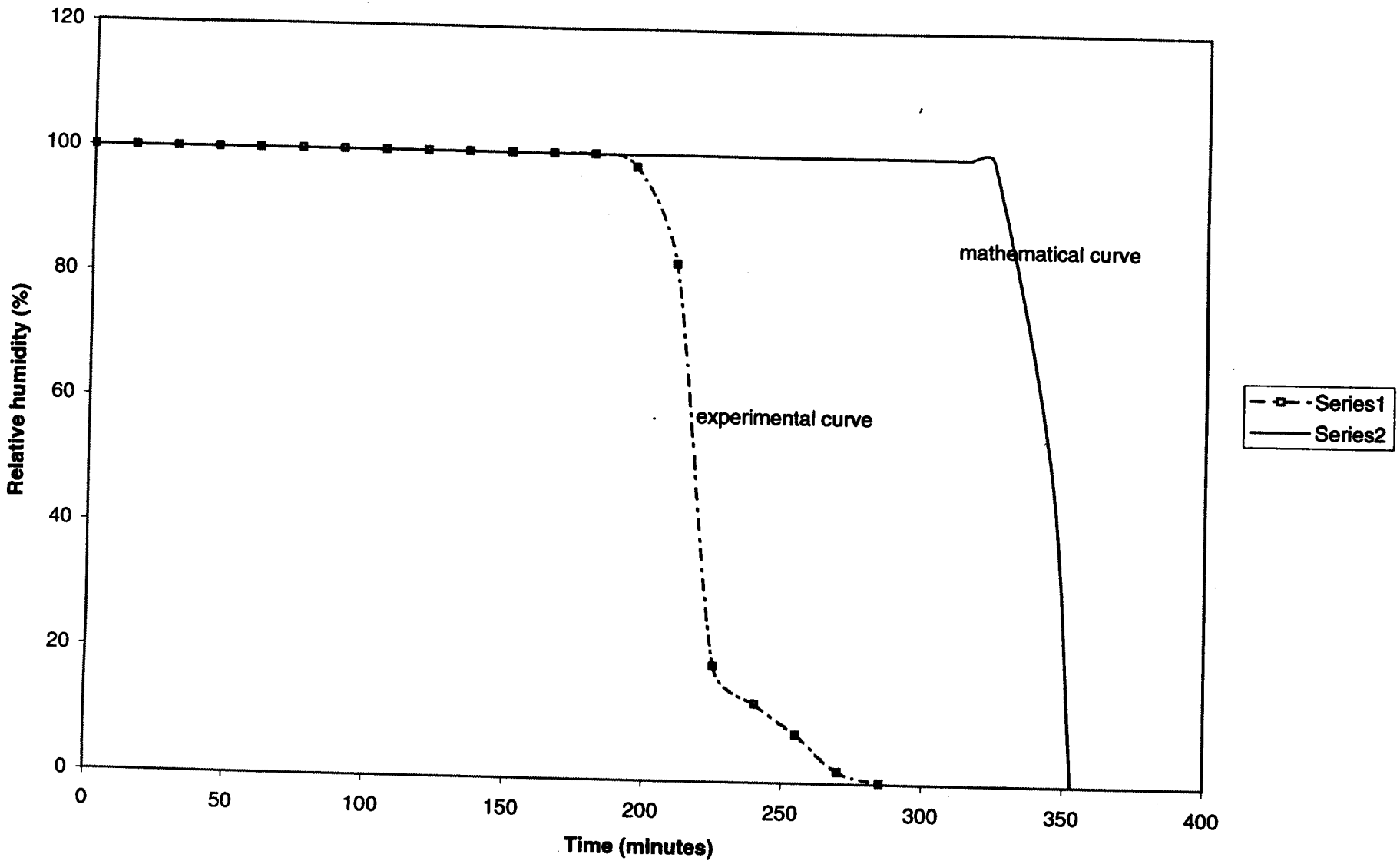

Figure 5.9 Comparison of drying rate curves

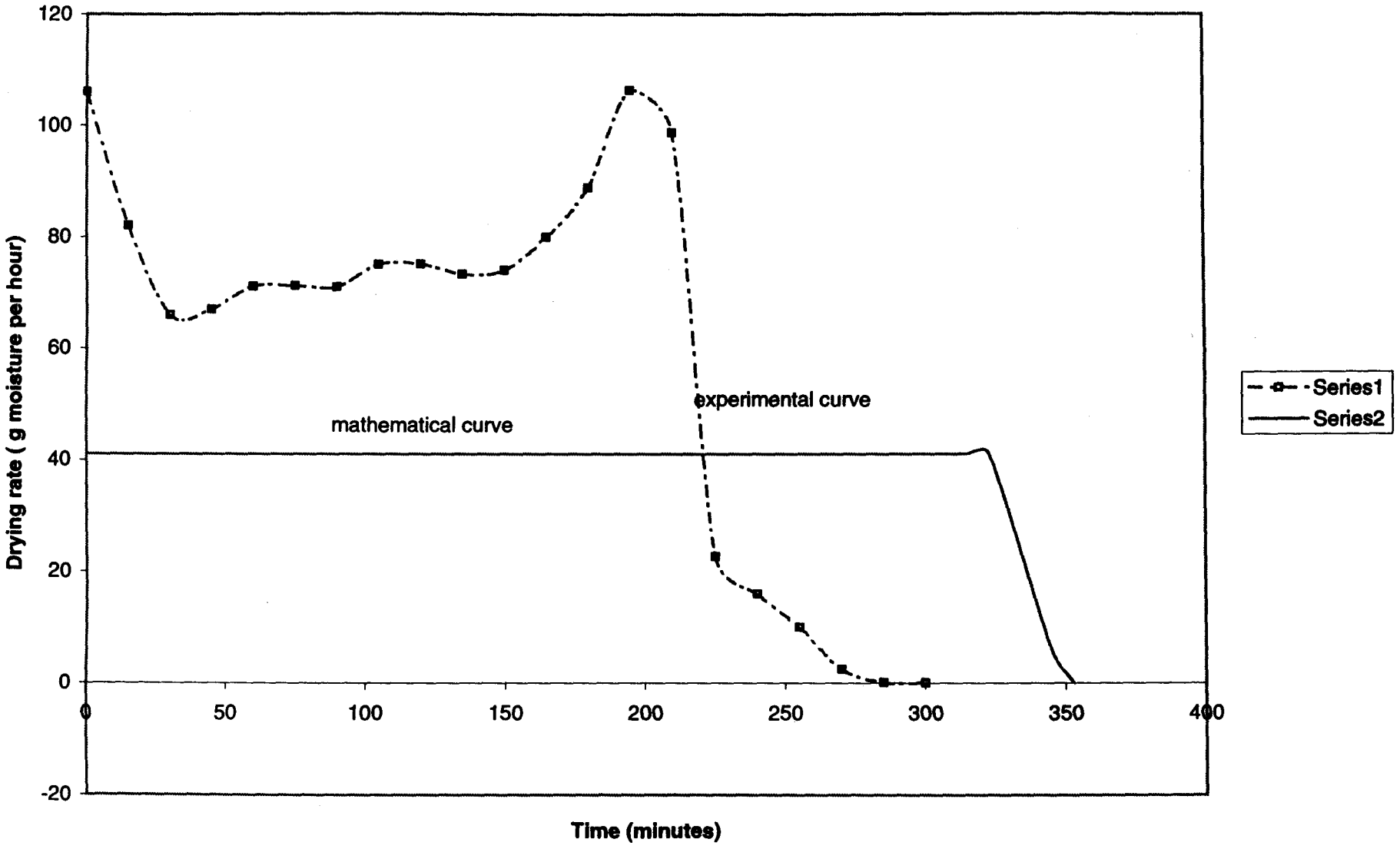

Figure 5.10 Comparison of product moisture content curves

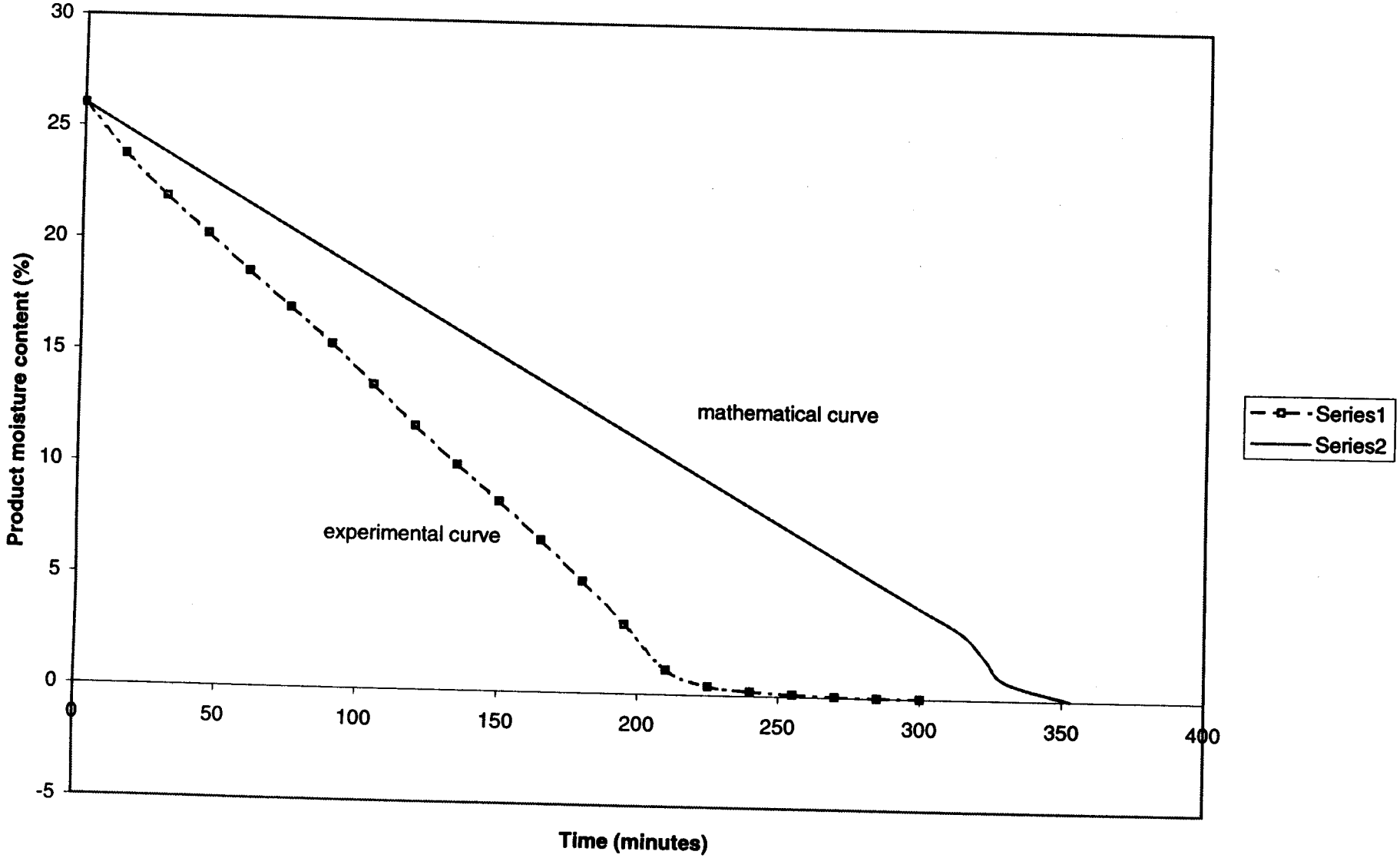

markers). When the moisture content is higher than 5%, which is the critical moisture content, the curve is a straight line. If the moisture content is below 5%, the slope of the curve will be smaller since the drying rate decreases.

The mathematical moisture content curve has the same trend as the experimental curve. Due to its lower constant rate, the slope of its constant part is smaller. But in the decreasing-rate stage, the moisture content drops faster because of a relative higher drying rate.

Inlet air Temperature	Vacuum level	Bleeding rate	Experimental results	Theoretical results	error
50°C	0.5 atm	8.5 m^3/h	3.72 hours	4.76 hours	+27.90%
40°C	0.5 atm	8.5 m^3/h	6.67 hours	5.87 hours	-12.01%
30°C	0.5 atm	8.5 m^3/h	6.37 hours	7.26 hours	+13.90%
20°C	0.5 atm	8.5 m^3/h	5.23 hours	9.71 hours	+85.60%
50°C	0.87 atm	3.4 m^3/h	15.75 hours	8.52 hours	-45.90%
40°C	0.87 atm	3.4 m^3/h	11.63 hours	10.17 hours	-12.50%
30°C	0.87 atm	3.4 m^3/h	12.5 hours	12.15 hours	-2.89%
20°C	0.87 atm	3.4 m^3/h	16.75 hours	14.55 hours	-13.10%

Table 5.3 Comparsion between mathematical and experimental results

For a PharmSep 12", with the same slurry weight, solid particles and inlet air humidity, the total drying time obtained from experiments were compared with mathematical calculations in Table 5.3. It is found that the error is pretty large. But from Table 5.2, with a 50°C, 8.5m^3/h inlet air and 0.5 atm vacuum level, the uncertainty of the drying time could be as large as 83.2%, but here the error is 27.9%. Therefor the results are still reasonable. The reasons causing errors include:

First, the exit air temperature is higher than the wet-bulb temperature. The actual drying process is not adiabatic, there is heat generated due to the vibration and heat may also be transferred from the environments to the drying system.

Second, the temperature of the product may be higher than the wet-bulb temperature due to the heat generation, thus the actual drying rate may not be as high as mathematical prediction.

Another reason is that, some parameters were not determined accurately in the mathematical calculations, such as heat/mass transfer area, heat transfer coefficient.

Uncertainty of the experimental data is also a reason causing errors. As mentioned in Section 5.1.4, the uncertainties of total exit air pressure, exit and inlet air humidity may cause the uncertainty of the drying rate.

To predict the results more accurately, it is necessary to estimate the total heat generation caused by vibration, and then estimate the actual exit air temperature in the constant-rate stage. For example, if the output of a vibrating device is 500 Watts, assuming 5% of its output may cause the increase of the exit air temperature, with Equation (5.1), the enthalpy of the actual exit air could be estimated. With a psychrometric chart, the exit air temperature could be obtained.

For the drying process shown in Figure 5.3, if heat generation due to the vibration was considered, the exit air temperature could be 14 °F higher than wet-bulb temperature. The modified exit air temperature curve was compared with experimental curve and mathematical curve in Figure 5.11. The modified exit temperature was closer to the actual case.

Modified drying rate curve was plotted in Figure 5.12. Compared with experimental curve, its constant drying rate is much closer to the actual drying rate, but its decreasing-rate is relative higher. Its total drying time is shorter but is closer to actual drying time.

To predict the drying rate process well, a relative accurate critical moisture content is also important to this model. For SWECO PharmAseps, we consider the critical moisture content is reached if there is no visible water in the vacuum line.

Figure 5.11 Modified exit air temperature curve

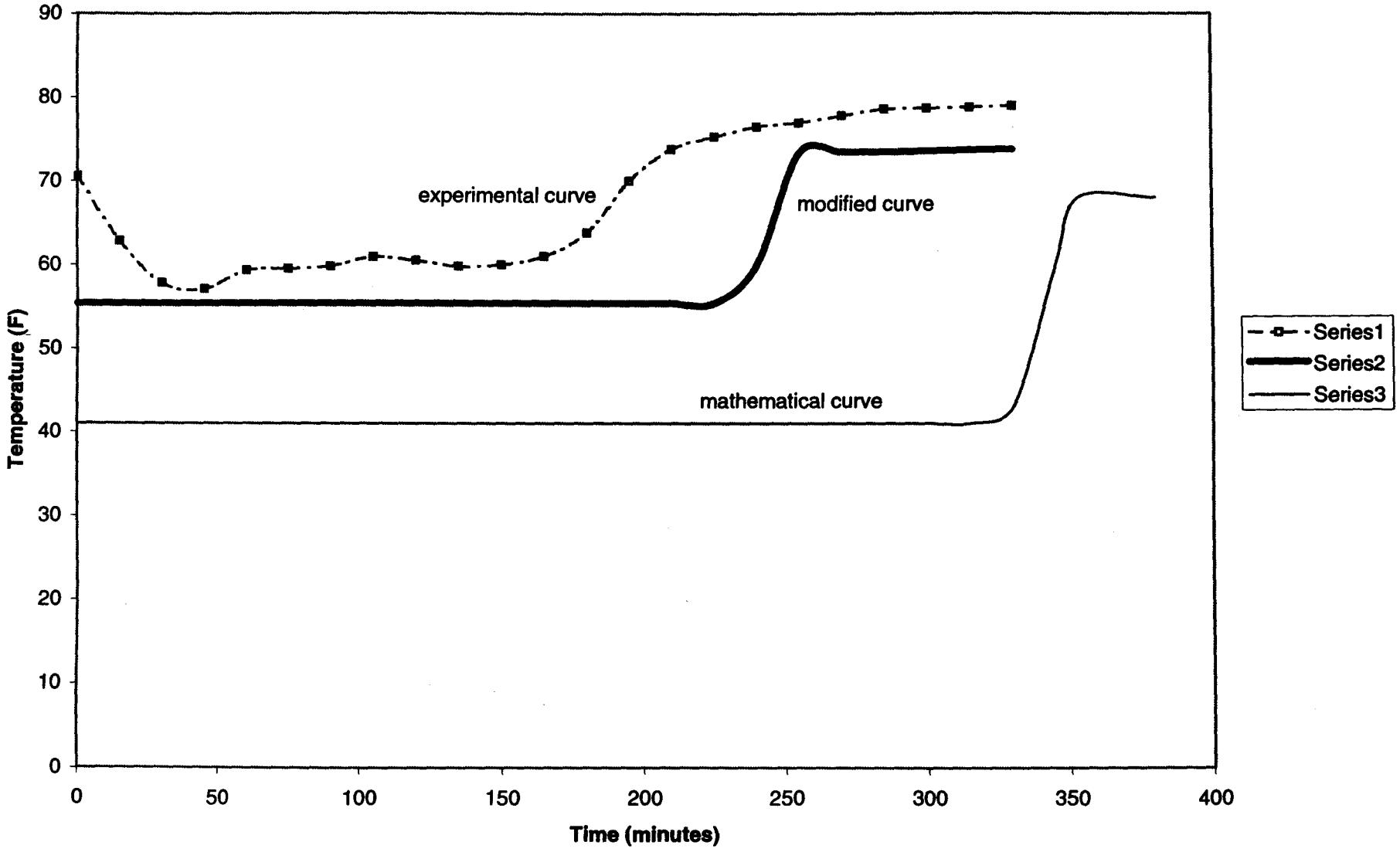

Figure 5.12 Modified drying rate curve

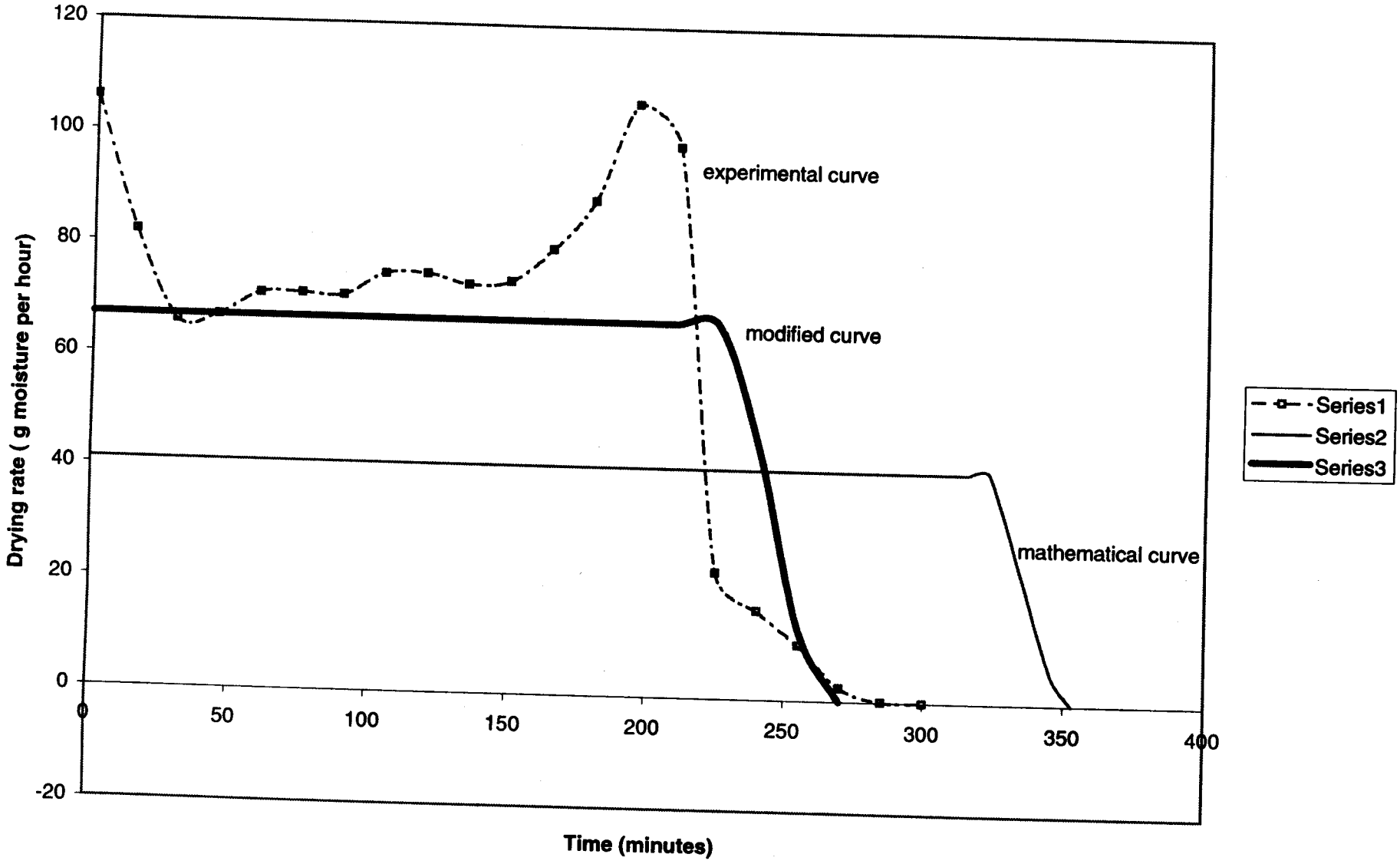

Chapter 6 Discussion

To optimize the performance of the separator, it is necessary to study the effect of following factors: air bleeding rate, exiting air humidity, vacuum level introduced, size of the particles, vibration frequency and amplitude, critical moisture content and heat exchange between the environment and the whole drying system.

6.1 Air Bleeding Rate

As mentioned in Chapter 3, increasing air bleeding rate can greatly increase the effective length of the capillary channels inside the wet product and thus increase the effective heat/mass transfer area. So the larger the air bleeding rate, the higher the drying rate.

If the air-bleeding rate is large enough so that the air can pick up all the evaporated moisture immediately, the effective length could be the whole thickness of the product cake and increasing the air bleeding rate would not be able to change the heat/mass transfer area any more.

Air bleeding rate may also influence the heat transfer coefficient and will assist the particles to remain clear from the product screen. The velocity of the particles may be affected by bleeding air velocity, so the heat transfer coefficient and drying rate. It can be seen from Equation (3.12), (3.13), (3.14), that regardless of the type of convective drying method used, the higher the air bleeding rate, the larger the heat transfer coefficient and thus the higher the drying rate.

6.2 Air humidity at the exit

The drying process occurs when the vapor pressure of water above the product particles is higher than the vapor pressure in the bleeding air. The vapor pressure above the product is determined not only by the temperature but also by the chemical and physical properties of the product particles, by the moisture content of the product and by the way in which water is bonded with the product particles.

In the constant drying stage, since the product is wet enough, the vapor pressure above the product is the saturated vapor pressure and the effective length doesn't occupy the whole thickness of the capillary channels and the air humidity at the exit may achieve 100%. But in the decreasing-rated stage, with a decreasing drying rate, the effective length becomes longer and longer till it occupies the whole thickness of the product cake. Now exit air humidity begins to decrease and its temperature begins to increase. At the same time, the vapor pressure above the product surface also decreases since the moisture content of the product is decreasing. This also causes the decreasing of the exit air humidity to decrease.

The variations of the exit air humidity and temperature for a 12" separator are shown in Figure 5.2. At exit, air relative humidity remained at 100% during the constant rate stage, then it decreased sharply because of the decreasing drying rate at the air-solid interface and the increasing exit air temperature. Exit air humidity may decrease below 1%. It is suggested to decrease the air bleeding rate when exit air humidity decreases to some degree. This measure can save energy without influence the drying rate obviously.

6.3 Role of Vacuum

If vacuum is introduced in the separator, the wet-bulb temperature decreases, and consequently the pressure decreases. For example, at one atmosphere pressure, the wet-bulb temperature of a 30°C dry air is 10 °C, but at one-fifth atmosphere pressure, the wet-bulb temperature of the 30°C dry air is –4.5°C. Since wet-bulb temperature decreases with vacuum, equations (3.1) and (3.5), the drying rate will increase greatly if high vacuum is introduced (assuming the freezing can be avoided).

But since the operating temperature of the product will decrease, sometimes the product will "freeze" during the drying process.

6.4 Critical Moisture Content

When the moisture content of the product decreases to a certain value, called critical moisture content, the drying rate decreases. To determine the drying time by using equation (3.11), we need to know the critical moisture content, X_C. It is quite difficult to determine the value of X_C except experimentally. The factors that will influence it include evaporating rate, thickness of the product cake and physical/chemical properties of the particles. If the evaporating rate is too high, evaporating surface will draw back inside the product at higher product moisture content, and the critical moisture content will be higher. Also in case the thickness of the product cake is large, the resistance to the capillary flow will be large, and thus the critical moisture content will increase.

Researchers in Tsinghua University provided following profiles of the critical moisture content of some kinds of materials. (Shown as Table 6.1, also seen in Reference 21)

Material Properties			Purging air Properties			Critical moisture content (kg moisture/kg dry product)
Name	Bed Thickness	Particle diameter	Velocity	Temperature	Humidity	
Sand	25 mm	<0.044 mm	2.0 m/s	54 °C	17%	0.21
Sand	25 mm	0.044~0.074mm	3.4 m/s	53 °C	14%	0.10
Sand	25 mm	0.149~0.177mm	3.5 m/s	53 °C	15%	0.053
Sand	25 mm	0.208~0.295mm	3.5 m/s	55 °C	17%	0.053
Soil	0.4 mm	NA	1.0 m/s	37 °C	10%	0.11
Soil	15.9 mm	NA	1.0 m/s	32 °C	16%	0.13
Soil	25.4 mm	NA	10.6 m/s	25 °C	40%	0.17
Leather	10 mm	NA	1.5 m/s	49 °C	NA	1.25
Wood	25 mm	NA	4.0 m/s	22 °C	34%	1.28
Wool	NA	NA	NA	25 °C	NA	0.31
$CaCO_3$	31.8 mm	NA	1.0 m/s	39 °C	20%	0.084

Table 6.1 Critical moisture content of some materials

From Table 6.1, it is obvious that the critical moisture content has a close relationship with the properties of the product particles. Because smaller particles have larger surface area, the corresponding critical moisture content would be higher. As pointed out in Chapter 2, if the microscopic pores inside the product are large enough, the vapor pressure above the product surface can be approximated as the saturation pressure, or it will be lower than the saturation pressure.

During the constant drying rate stage, since the drying surface can be treated as free evaporation surface, the vapor pressure above the product surface should be kept as the saturation pressure, or the dry rate will decrease. Thus, during the constant rate stage,

only adsorbed moisture and part of capillary moisture can be removed. To remove more capillary moisture and in-depth moisture, the drying rate will decrease. That is why for some product, such as leather and wood, their critical moisture contents are so high.

For the sanitary separators which we used in these experiments, critical moisture content is influenced by three main factors: (1) Type and size of the separator, (vibration energy of the unit and surface area of the screen) (2) properties of the product particles and (3) level of vacuum introduced. By experimentally measuring the drying time, Equation (3.11) can be used to calculate the critical moisture content.

6.5 Effect of the vibration

By vibrating the product screen, the particles can be suspended above the product screen. Vibration will help to overcome the energy that bounds the moisture and particles together and greatly increases the velocity of the moving particles. This will increase the drying rate and decrease the drying time.

6.6 Diameter of Particles

The diameter of the product particles will affect the heat transfer coefficient, from Equation (3.14). The smaller the diameters of particles, the higher the heat transfer coefficients and thus the faster the drying rate.

As mentioned in Section 6.4, the diameter of particles (total surface area) will also affect the binding of water with the particles, the smaller the particles, the higher the critical moisture content.

In addition, the smaller the particles, the larger the mass/transfer area and thus higher drying rate during the constant drying stage. But since smaller size particles cause higher critical moisture content, sometimes drying smaller particles may cost more time for drying.

6.7 Influence of the environment temperature

The model described in Chapter 3 is based on the assumption the whole drying process is adiabatic, there is no heat exchange between the drying system and the environment. But in fact, this kind of exchange can not be avoided. As pointed out in Section 6.3, the product temperature may decrease below freezing point in case of application of high vacuum. But in fact, it is not easy for the product to reach such a low temperature, the heat exchange may occur and the actual drying rate will not be as fast as predicted.

But this heat exchange may also warm the drying air and increase its ability to pick up the evaporated moisture. From this point of view, heat transferred from the environment can increase the drying rate. This heat exchange is most pronounced in Jacketted units.

Chapter 7 Recommendations and Conclusion

This thesis describes a simple mathematical model used to predict the drying time in a vibrating separator. This model determines the rate of evaporation as air is forced through a screen and passes through a wet product cake that is accumulated and vibrated above the product screen. This model assumes that the whole drying process is adiabatic and predicts the drying time on the basis that some parameters, such as critical moisture content X_c and heat transfer coefficient α, can be determined by experiments or by semi-empirical correlations.

Chapter 5 demonstrates that for such a simplistic model, the drying time for product particles can be reasonably predicted. The difficulty is in general applications of this model to different models of separators and different products. If this model is used for a different powder or separators, new experiments should be adopted to determine the critical moisture content, X_c. It is probable that diffusive resistance, s/keff, and the convection heat transfer coefficient, α, should also be empirically determined for the new powder and/or separator. Since the users of this model are usually users of the vibro-separators and may not be familiar with the experimental procedures, they may have difficulties during their predictions. And, in addition, it may not be economically feasible for them to do these preliminary tests.

To eliminate the inconvenience caused by these experiments, a probable option is to develop a more detailed numerical model. This model would no longer use a simple thermal resistance analogy to predict the rate of heat transfer. Instead the rate of the heat transfer would be determined from solving the Navier-Stokes and energy equations.

Although the current simple model can still be used and X_c, s/keff and α can be determined from the detailed model, the advantage of this new approach is that the empirical parameters such as X_c, s/keff and α, would no longer be required. Aside from being academically more satisfying, this should eliminate the need for experiments in order to make predictions.

The major difficulty in implementing such a numerical solution is determining how to theoretically determine effect of the vibrating powder/water slurry. One possibility is to use a volume-averaging approach such as is used for porous media. Although this approach should eliminate the need to empirically determine X_c and perhaps α, an effective thermal conductivity very similar to that used in s/keff may be required. We should be able to predict this value from semi-empirical correlations from the literature.

Some type of lumped powder/water volume elements should work well for performing energy balances and predicting evaporation rates.

The primary drawback to attempting this detailed model is that there is no guarantee that it will more accurately predict the drying time.

So, it is a classical high-risk problem but if successful it will eliminate the need for empirical parameters and experiments.

In this thesis, I use the glass beads as the product particles and experimentally determined the empirical parameters (X_c, α) to obtain mathematical prediction with the current model. The experimental results show that the predictions from this current model are fairly accurate. In fact, the advantage of the current model is that, in case of empirical determination of parameters are relatively insensitively to changes in powder and/or

separators, the current model can predict the results rather accurately and could be applied more widely.

Reference

[1] Stanislav, J F. *Mathematical Modeling of Transport Phenomena Process* Ann Arber Science 1982.

[2] Perry, J.H., D.W.Green, *Perry's Chemical Engineers Handbook*, 6th, McGraw Hill, 1984.

[3] Earle, R L. *Unit Operations in Food Processing*, Pergamon Press, 1985.

[4] Davison, J F. and Harrison, D. *Fluidization,* Academic Press, 1971.

[5] Rich, L G. *Unit Operation of Sanitary Engineering*, John Wiley & Sons, Inc., 1961.

[6] Rudobashta, SP. Malygin, E N. Kuz'mina, N V and Shadrina, NE, "Mathematical simulation and optimization of convective drying", 1990. "*Theoretical Foundations of Chemical Engineering (English Translation of Teoreticheskie Osnovy Khimicheskoi Tekhnologii).*" v 23 n 3, p210-214.

[7] Sun, Ssu-Hsueh. Marrero, Thomas R. "Experimental study of simultaneous heat and moisture transfer around single short porous cylinders during convection drying by a psychrometry method" 1996 "*International Journal of Heat and Mass Transfer*". v 39 n 17 p 3559-3565.

[8] Derdour, L. Desmorieux, H. Andrieu, J. "Determination and interpretation of the critical moisture content (C.M.C.) and the internal moisture content profile during the constant drying rate period" 1998. "*Drying Technology*". v 16 n 3-5. P813-824.

[9] Masmoudi, W. Prat, M. "Heat and mass transfer between a porous medium and a parallel external flow. Application to drying of capillary porous materials." 1991. "*International Journal of Heat and Mass transfer*". v 34 n 8 p 1975-1989.

[10] Murugesan, K. Seetharamu, K N. Narayana, P A Aswatha. "One dimensional analysis of convective drying of porous materials" 1996. "*Warme und Stoffubertragung-Thermo & Fluid Dynamics*". v 32 n 1-2. P81-88.

[11] Olivierira. Leandro S. Haghighi, Kamyar. "Conjugate heat and mass transfer in convective drying of porous media". 1998. "*Numerical Heat Transfer Part A-Applications*". v 34 n 2 p 105-117.

[12] Wang, Zhaohui. Fu, Jie. "Simplified drying model of heat and mass transfer". 1995. "*Huagong Xuebao/Journal of Chemical Industry & Engineering(China)*". v 46 n5 p 579-585.

[13] Zhang, Zhe. Yang, Shiming. "Mechanism and mathematical model of heat and mass transfer during convection drying of porous media". 1997. "*Huagong Xuebao/Journal of Chemical Industry & Engineering(China)*". v 48 n1 p 52-59.

[14] Rogers, J. Kaviany, M. "Variation of heat and mass transfer coefficients during drying of granular beds". 1990. "*American Society of Mechanical Engineering, Heat Transfer Division, (Publication) HTD.*". v 101. P153-163.

[15] Nedeljkov, Mita I. Stakic, Momir P. "Mathematical modeling of convective drying processes for granular materials". 1989. "*First International Forum on Mathematical Modeling Computer Simulation of Processes in Energy Systems.*" Sarajevo, Yugoslovia.

[16] Nasrallah, S Ben. Perre, P. "Detailed study of a model of heat and mass transfer during convective drying of porous media". 1988. "*International Journal of Heat & Mass Transfer*". v 31 n 5 p957-967.

[17] Fudym, O. Carrere-gee, C. Dufresne, J L. Lahellec, A. Lecomte, D. "TEF approach: application to parameter estimation in drying". 1998. "*Theory and Practice Proceedings of the international Conference on inverse Problems in Engineering 1998. ASME, Fairfield, NJ, USA.*" p 447-454.

[18] Marinos-Kouris, D. Maroulis, Z B. Kiranoudis, C T. "Modeling, simulation and design of convective industrial dryers". 1998. "*Drying Technology*". v 16 n 6 p 993-1026.

[19] Mazyak, Z Yu. Il'kiv, I N. "Heat and mass transfer in convective variable-temperature drying" 1992. *"Heat Transfer Research"*. v 24 n 8, p 1052-1057.

[20] Fernandez, Melvyn L. Howell, John R. "modeling of convective drying of porous materials". 1996. *"Porous Flow Heat Transfer American Society of Mechanical Engineers. Heat Transfer Division. (Publiscation) HTD"*. v 331 1996. ASME, New York, NY, USA. p 3-14.

[21] Jiang, Weijun. Lei, Liangheng. Liu, Maolin. *"Unit Operations of Chemical Engineering/ Hua Gong Yuan Li (China)"*. Tsinghua University Press, 1993.

[22] Sattler, Klaus. Feindt, Hans Jacob. *"Thermal Separation Process"*. VCH, 1995.

[23] Hazrati, Azar. *"Test Results of Drying on screen of SWECO PharmASep Optimization of Drying Circle By Controlling the Purging Air and Vacuum"*, 1999.

Appendix I Partial vapor pressure of water vapor

temp	Ps.t	temp	Ps.t	temp	Ps.t	temp	Ps.t
C	mbar	C	mbar	C	mbar	C	mbar
-20	1.02	-2	5.16	16	18.13	34	53.07
-19	1.13	-1	5.61	17	19.32	35	56.1
-18	1.25	0	6.09	18	20.59	36	59.26
-17	1.37	1	6.56	19	21.92	37	62.6
-16	1.5	2	7.04	20	23.31	38	66.09
-15	1.65	3	7.57	21	24.8	39	69.75
-14	1.81	4	8.11	22	26.37	40	73.58
-13	1.98	5	8.7	23	28.02	41	77.59
-12	2.17	6	9.32	24	29.77	42	81.8
-11	2.37	7	9.99	25	31.6	43	86.18
-10	2.59	8	10.7	26	33.53	44	90.79
-9	2.83	9	11.46	27	35.56	45	95.6
-8	3.09	10	12.25	28	37.71	46	100.61
-7	3.36	11	13.09	29	39.95	47	105.87
-6	3.67	12	13.99	30	42.32	48	111.33
-5	4	13	14.94	31	44.82	49	117.07
-4	4.36	14	15.95	32	47.43	50	123.04
-3	4.75	15	17.01	33	50.18	51	129.69

Note:
(1) $P_{s.t}$ is partial pressure of the water vapor at temperature t.
(2) Abridged from Keenan,J.H., F.G.Keyes, P.G.Hill, and J.G.Moore, "steam Tables", John Wiley&Sons, Inc. New York. 1969

Appendix II Psychrometric Chart

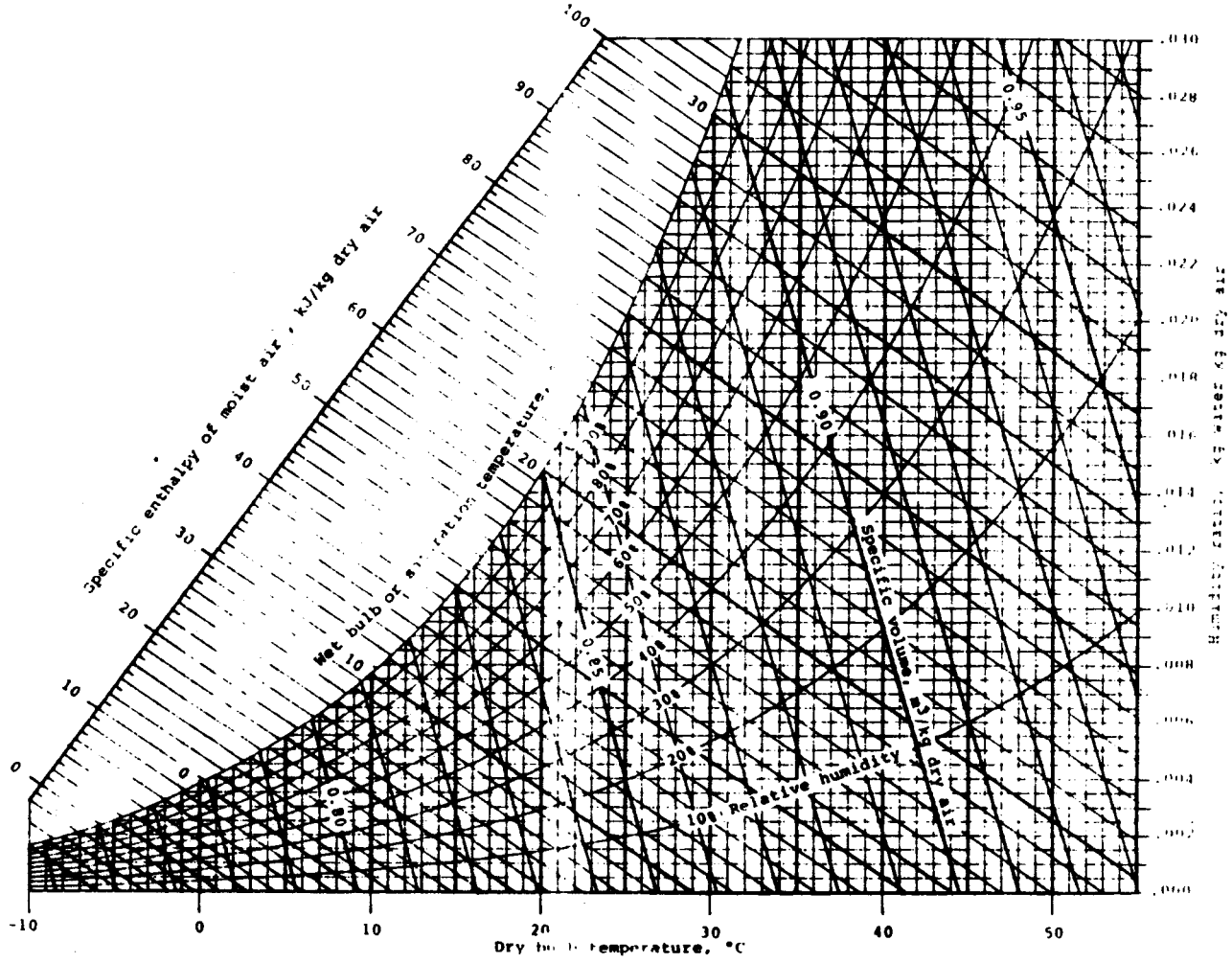

Appendix III A Visual Basic Program (main function)

```
Private Sub Command1_Click()
End
End Sub

Private Sub Command2_Click()
Welcome.Hide
cmc.Show
End Sub

Private Sub cmdCalcul_Click()
Dim pst(200) As Double
Dim alfa As Double
Dim d As Double
Dim velo As Double
Dim vicous As Double
Dim t As Integer
Dim h As Double
Dim i As Double
Dim i1 As Double
Dim i2 As Double
Dim tw As Integer
Dim p As Double
Dim G As Double
Dim GT As Double
Dim Xc As Double
Dim Time As Double
Dim X As Double
Dim A As Double
Dim hfg As Double
Dim dt As Double
Dim conduct As Double
Dim ddt As Double
Dim thick As Double
Dim density As Double
Dim time1 As Double
Dim time2 As Double
Dim sa As Double
Dim dscreen As Double
Dim abrate As Double
Dim ta As Integer
Dim hum1 As Double
Dim hum2 As Double
Dim tw1 As Double


If help.Check1 = 1 Then
dscreen = 30.5
Else
If help.Check2 = 1 Then
dscreen = 45.7
Else
If help.Check3 = 1 Then
dscreen = 76.2
```

```
Else
If help.Check4 = 1 Then
dscreen = 116.8
Else
If help.Check5 = 1 Then
dscreen = 152.4
End If
End If
End If
End If
End If


d = CDbl(Step1.txtDiameter.Text) * 0.001
velo = CDbl(Step1.txtVelo.Text)
viscous = CDbl(Step2.txtViscous.Text) * 0.000001
t = CInt(Step2.txtTemp.Text)
h = CDbl(Step2.txtHum.Text) / 100
p = CDbl(Step2.txtVacu.Text)
hfg = 2400.1 * 1000
A = 3.14 * (dscreen / 100) ^ 2 / 4
G = CDbl(slurry.txtG.Text) - CDbl(slurry.Text2.Text)
GT = CDbl(Step1.txtGT.Text)
conduct = CDbl(Step1.conduct.Text)
Xc = CDbl(cmc.txtXC.Text)
density = CDbl(Step1.Text1.Text)
abrate = CDbl(Step2.Text1.Text)


pst(100) = 123.04
pst(99) = 117.07
pst(98) = 111.33
pst(97) = 105.87
pst(96) = 100.06
pst(95) = 95.6
pst(94) = 90.79
pst(93) = 86.18
pst(92) = 81.8
pst(91) = 77.59

pst(90) = 73.58
pst(89) = 69.75
pst(88) = 66.09
pst(87) = 62.6
pst(86) = 59.26
pst(85) = 56.1
pst(84) = 53.07
pst(83) = 50.18
pst(82) = 47.43
pst(81) = 44.82

pst(80) = 42.32
pst(79) = 39.95
```

pst(78) = 37.71
pst(77) = 35.56
pst(76) = 33.53
pst(75) = 31.6
pst(74) = 29.77
pst(73) = 28.02
pst(72) = 26.37
pst(71) = 24.8

pst(70) = 23.31
pst(69) = 21.92
pst(68) = 20.59
pst(67) = 19.32
pst(66) = 18.13
pst(65) = 17.01
pst(64) = 15.95
pst(63) = 14.94
pst(62) = 13.99
pst(61) = 13.09

pst(60) = 12.25
pst(59) = 11.46
pst(58) = 10.7
pst(57) = 9.99
pst(56) = 9.32
pst(55) = 8.7
pst(54) = 8.11
pst(53) = 7.57
pst(52) = 7.04
pst(51) = 6.56

pst(50) = 6.09
pst(49) = 5.61
pst(48) = 5.16
pst(47) = 4.75
pst(46) = 4.36
pst(45) = 4
pst(44) = 3.67
pst(43) = 3.36
pst(42) = 3.09
pst(41) = 2.83

pst(40) = 2.59
pst(39) = 2.37
pst(38) = 2.17
pst(37) = 1.98
pst(36) = 1.81
pst(35) = 1.65
pst(34) = 1.5
pst(33) = 1.37
pst(32) = 1.25
pst(31) = 1.13
pst(30) = 1.02

alfa = 0.0259 * (2 + 0.54 * Sqr(d * velo / viscous)) / d
i = 1.005 * CDbl(t) + 0.622 * h * pst(t + 50) * (2500 + 1.84 * CDbl(t)) / (1000 * (1 - h * pst(t + 50) / 1000))

```
 For j = t To -30 Step -1
 i1 = 1.005 * CDbl(j) + 0.622 * pst(j + 50) * (2500 + 1.84 * CDbl(j)) / (1000 * (p - pst(j + 50) / 1000))
 i2 = 1.005 * CDbl(j - 1) + 0.622 * pst(j + 49) * (2500 + 1.84 * CDbl(j - 1)) / (1000 * (p - pst(j + 49) /
 1000))
 If (i - i2) = (i1 - i) Then
   tw = (2 * CDbl(j) - 1) / 2
   Else
   If i2 < i And i < i1 And (i - i2) < (i1 - i) Then
   tw = CDbl(j) - 1
   Else
   If i2 < i And i < i1 And (i - i2) > (i1 - i) Then
   tw = CDbl(j)
   End If
   End If
   End If
  Next j

 X = (G - GT) / GT
 dt = t - tw
 ddt = dt / 1000
 thick = d * 100

 hum1 = 0.622 * h * pst(t + 50) / (1000 - h * pst(t + 50))

 If exitair.Check1 = 0 Then
 ta = CDbl(exitair.Text1.Text)
 hum2 = 0.622 * pst(ta + 40) / (p * 1000 - pst(ta + 40))
 Else
  'If tw < -10 Then
   'tw1 = 5
   'Else
    'If tw < -5 Then
    'tw1 = 10
    'Else
     'If tw < 0 Then
     'tw1 = 15
     'Else
      'If tw < 5 Then
      'tw1 = 20
      'Else
        'tw1 = tw + 10
    'End If
   'End If
  'End If
 'End If

 hum2 = 0.622 * pst(tw + 58) / (p * 1000 - pst(tw + 58))
 End If

 If G <= (Xc + 1) * GT Then
 time1 = 0
 Else
 time1 = (G - (Xc + 1) * GT) / (abrate * 1.29 * (hum2 - hum1))
 'time1 = (G - (Xc + 1) * GT) * hfg * 1000 / (0.25 * A * 3600 * alfa * ddt * 1000)
```

```
End If

For j = 1 To 999
sa = 1 / alfa + thick * j / (1000 * conduct)
If X < Xc Then
dtime = 0.001 * X * GT * sa * hfg / (0.25 * A * 3600 * dt)
Else
dtime = 0.001 * Xc * GT * sa * hfg / (0.25 * A * 3600 * dt)
End If
time2 = time2 + dtime
Next j

Time = time2 + time1


txtOutput.Text = CStr(time1)

End Sub
```